School of Biochemistry and Immunology

Trinity College Dublin

Thermoregulation in the Brain and Body: Understanding the Influence of Memory on Innate Responses

By

Lydia C. Marks

A Dissertation

Presented to the University of Dublin, Trinity College

in fulfilment of the requirement for the degree of Research Masters

Master of Science in Biochemistry

Supervisor: Dr. Tomás Ryan

2021

Declaration

I declare that this thesis has not been submitted as an exercise for a degree at this or any other university and it is entirely my own work.

I agree to deposit this thesis in the University's open access institutional repository or allow the library to do so on my behalf, subject to Irish Copyright Legislation and Trinity College Library conditions of use and acknowledgement.

Name: Lydia Marks

Date: 2021

Abstract

Thermoregulation is the ability for an organism to maintain a specific internal temperature while existing in an environment with constantly changing external temperatures. This is a critical homeostatic response and the inability to thermoregulate can be life-threatening. Therefore, understanding the thermoregulatory system within mammals has been pertinent to biological research for centuries. The brain plays a crucial role in sensing temperature changes and initiating the appropriate thermoregulatory responses. Recent technological developments have enabled the investigation of neuronal mechanisms driving innate thermoregulatory responses. This project aims to further our understanding of the components influencing thermoregulation. Engram labelling technology, originally used in memory research, will be optimised to label and manipulate the specific temperature-sensitive neurons within the brain. This research will also investigate whether innate thermoregulatory responses can be modulated by learning and memory. The aim is to further our understanding of the relationship between learned and innate responses.

Acknowledgements

I would like to thank Dr. Tomás Ryan for his scientific guidance, support, critical feedback, and expertise throughout this research project. I would also like to thank Dr. Lydia Lynch for providing feedback and expertise on the metabolic aspect of this project.

I would also like to thank Aaron Douglas, Dr. Clara Ortega-de-san-Luis, Sarah Power, Dr. James O'Leary, Livia Autore, Antoine Harel, and Dr. Maurizio Pezzoli for teaching me all of the techniques used in this research and for providing scientific knowledge, support, and advice every step of the way.

I would also like to thank the Comparative Medicines Unit staff for providing care of the animals used in this project.

This research project would not be possible if it were not for the assistance and guidance provided by each of the individuals listed above.

Table of Contents

Table of Figures

Abbreviations

AAV	Adeno-Associated Viruses
BAT	Brown Adipose Tissue
BDNF	Brain-Derived Neurotrophic Factor
ChR2	Channelrhodopsin-2
CO_2	Carbon Dioxide
CSN	Cold-Sensitive Neurons
Dox	Doxycycline
EE	Energy Expenditure
EYFP	Enhanced Yellow Fluorescent Protein
iBAT	Intrascapular Brown Adipose Tissue
IEG	Immediate Early Gene
MnPO	Median Preoptic Nucleus of the Hypothalamus
NST	Non-Shivering Thermogenesis
POA	Preoptic Area of the Hypothalamus
RQ	Respiratory Quotient
TNZ	Thermoneutral Zone
TRE	Tetracycline-Responsive Element
tTA	Tetracycline Transactivator
UCP-1	Uncoupling Protein-1
vLPO	Ventral Part of the Lateral Preoptic Nucleus
VMPO	Ventromedial Preoptic Area
WSN	Warm-Sensitive Neurons
4-OHT	4-Hydroxytamoxifen

Chapter 1: Introduction

1.1 Importance of thermoregulation in homeostasis

In biological systems, homeostasis is a dynamic equilibrium that is maintained to allow the optimal functioning of the organism. Maintaining homeostasis is critical for survival and it requires the precise regulation of numerous physiological variables. One of the most important homeostatic processes is thermoregulation, which is an organism's ability to maintain a specific internal temperature. The benefit of this is to provide a constant internal environment for cells and organs to function precisely, robustly, and efficiently despite a changing external environment (Liedtke, 2017).

Organisms are divided into two groups, ectotherms and endotherms, based on their strategies of thermoregulation (Shabtay and Arad, 2005). Ectotherms rely on external heat sources to thermoregulate, whereas endotherms use internal metabolic processes to regulate their temperature. Each species has a thermoneutral zone (TNZ), which is a specific range of temperatures where the animal's metabolic heat production and evaporative heat loss to the environment are in equilibrium (Hankenson et al., 2018). The present research focuses on endotherms, or "warm-blooded" animals, and the mechanisms and processes they employ to maintain thermoregulation.

For endothermic animals, the inability to maintain a core body temperature within the TNZ is life-threatening. Hyperthermia and hypothermia are conditions where the internal core temperature is extremely high or low, respectively. These conditions can be caused by extreme external temperatures that overwhelm the normal thermoregulatory mechanisms, resulting in an inability to produce or dissipate heat quickly enough to maintain a core temperature within the TNZ. Alternatively, hypothermia and hyperthermia can be caused by disruptions in the normal functioning of the thermoregulatory system, such as the inability to sense and react to temperature changes (Simon, 1993, Dhaka et al., 2006).

Most of our scientific interest arises from understanding thermoregulatory processes in humans; however research is not always possible in our species due to technical, ethical

or other reasons. Therefore, rodents have been used as a model organism to investigate and manipulate the circuits and systems driving thermoregulation. Even though many genetic, neuronal, and systemic aspects of thermoregulation are conserved between humans and rodents, there are also important differences between the two species that affect temperature regulation and must be addressed.

The main difference is the size of each species, where body surface area determines the amount of heat loss (Reitman, 2018). Since rodents are much smaller than humans, they lose a greater amount of heat to the environment and, therefore, must generate more heat to maintain thermoregulatory homeostasis (Reitman, 2018). To stay within their TNZ, mice prefer to be in an ambient environmental temperature of 30-31°C (Gordon et al., 1998). This allows them to maintain a core body temperature of 36-38°C, however their core temperature can oscillate depending on circadian rhythm, sex, and age (Hankenson et al., 2018, Tansey and Johnson, 2015).

1.2 Thermoregulatory mechanisms

When mice encounter environments outside their TNZ, they maintain thermoregulatory homeostasis through both behavioural and autonomic responses. Behavioural responses minimise energy expenditure while defending core body temperature (Hankenson et al., 2018). Common thermoregulatory behaviours that mice use include thermotaxis (movement towards or away from heat), postural changes (increasing or reducing exposed surface area), and altering microenvironments (huddling or nesting) (Gaskill et al., 2012, Hankenson et al., 2018, Tan and Knight, 2018). Mice also increase or decrease food consumption and locomotor activity to combat cold and warm environments, respectively (Terrien et al., 2011).

In addition to behavioural responses, mice also use autonomic responses to alter heat exchange between the mouse and its environment. One such response is the regulation of blood flow to the extremities, such as the tail and paws. Mice lose a lot of heat from their extremities due to the high surface area to volume ratio of these body parts (Hankenson et al., 2018). Therefore, in cold environments mice use peripheral vasoconstriction, or reduced blood flow to extremities, to reduce heat loss (Hankenson et al., 2018). In contrast, peripheral vasodilation, or increased blood flow to extremities,

allows mice to release body heat through the tail in response to warm environments. Rodents also respond to warm environments by invoking evaporative heat loss through spreading saliva across their body (Madden and Morrison, 2019).

Another critical autonomic response in warm-blooded animals is the ability to increase metabolic heat production in response to cold environments through a process called thermogenesis, which is divided into shivering and non-shivering thermogenesis (NST). Both types of thermogenesis are activated within minutes of exposure to a cold environment and the processes are dependent on metabolic mechanisms within specific tissues (Himms-Hagen, 2001). Shivering thermogenesis consists of fast, repeated skeletal muscle contractions that result in heat generation (Banet et al., 1978). This type of thermogenesis is effective in large mammals, but it is inefficient in rodents due to their relatively small muscle mass (Hankenson et al., 2018). Instead, rodents rely more on non-shivering thermogenesis, which occurs in Brown Adipose Tissue (BAT) and thus is also referred to as BAT thermogenesis.

The process of heat generation in BAT is fuelled by a mitochondrial protein, uncoupling protein-1 (UCP-1), that is unique to brown adipocytes, and its function is to transform the lipids accumulated from food into heat that can be released from the cell (Avram et al., 2005). Cold exposure triggers the release of norepinephrine, which mediates thermogenic activity mainly via β-adrenergic receptors (β-AR) (Quevedo et al., 1998). One method of measuring BAT thermogenesis is to quantify UCP-1 mRNA expression levels in BAT. For example, mice exposed to ambient cold (8°C) for 24 hours show increased UCP-1 expression in BAT compared to mice kept at room temperature (22°C) (Shore et al., 2013). However, only measuring UCP-1 mRNA levels can be misleading because the mRNA levels increase rapidly upon cold exposure, with peak expression occurring after 6 hours in the cold. The UCP-1 mRNA levels then decrease as the cold exposure continues throughout the following days and weeks. This would lead to the conclusion that the largest change in BAT occurs during acute exposure to cold, however in reality there are other changes that occur in BAT during the 3-5 weeks of cold exposure that facilitate increased thermogenic capacity (Nedergaard and Cannon, 2013, Cannon and Nedergaard, 2004).

1.2.1 Measuring thermogenesis using indirect calorimetry

Quantifying UCP-1 mRNA and protein levels provides us with important information about the presence and extent of BAT thermogenesis, however, it is only possible to collect and analyse this data post-mortem. To study thermogenesis *in vivo* we can use the non-invasive method of indirect calorimetry, which provides measurements that reflect changes in metabolic rate. The basal, or resting, metabolic rate is defined by the energy required to maintain normal functioning of a body at rest (Degen et al., 1998). There are various factors that determine the basal metabolic rate, including energy expenditure as a result of food consumption, energy used on physical activity, and energy used to maintain a core body temperature within the TNZ (Speakman, 2013). To measure the metabolic rate, we must measure the heat generated by an animal. However, it is very technically challenging to measure small amounts of heat, such as the amount a rodent might generate. Thus, researchers often use indirect calorimetry to measure components of the metabolic process instead of the heat generated (Speakman, 2013).

One such measurement used to gauge the metabolic rate of an animal is energy expenditure (EE), which represents the amount of calories used over a specific time period. There are various methods of calculating the EE but the majority take into account the respiratory quotient (RQ) and some methods correct for the estimated protein metabolism (Kaiyala et al., 2019, Weir, 1949). As temperature diverges from the TNZ (either higher or lower) the animal must expend more energy to maintain thermoneutrality. When the temperature is colder than the TNZ, the metabolic rate increases to match the heat lost to the environment (Riede et al., 2017).

Another way to measure metabolic rate is by calculating the carbon dioxide (CO_2) output from an animal. An increase in CO_2 emission signifies that an animal is performing cellular respiration at a faster rate (Raetz, 2015). An increased rate of CO_2 emission signifies a higher metabolic rate, whereas a lower output of CO_2 reflects a lower metabolic rate. In response to a cold environment, mice will increase their metabolic rate to fuel the cold-defensive responses, and therefore will show a higher output rate of CO_2.

When measuring an animal's metabolic rate there are normal variations based on a number of factors, including sex and circadian rhythm. Rodents are nocturnal and crepuscular and thus are more active just before, and during dark hours (Hawkins and Golledge, 2018). As a result, rodents exhibit higher metabolic rates and EE during their active hours, which correspond to the dark hours of the day (van der Vinne et al., 2015). It follows that core body temperature in mice is higher during the night time active phase than during the daytime inactive phase (Figure 1.2.1) (Gordon, 2017, Gordon, 2009). When mice are given a choice of temperature, they choose to stay at warmer ambient temperatures during the daytime when they are less active, and colder temperatures during their night time active phase (Gordon, 2017).

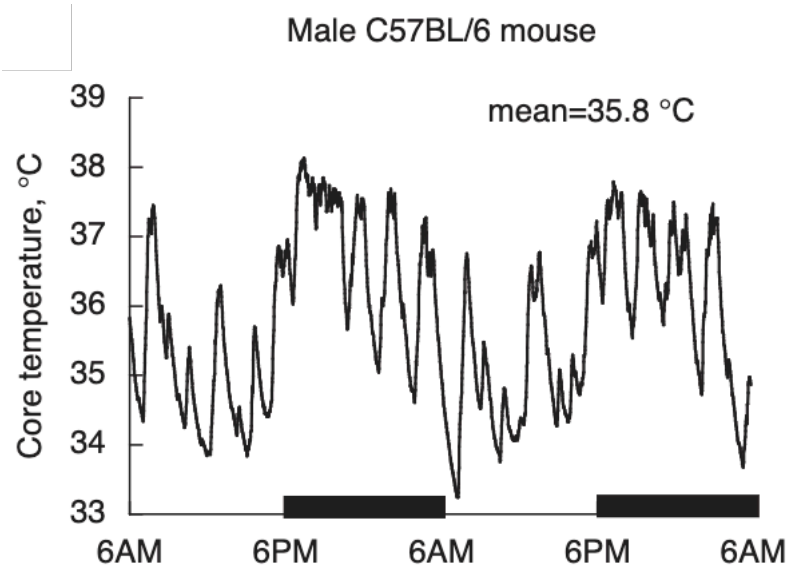

Figure 1.2.1: Natural fluctuations in male C57BL6 core body temperature across a 48 hour period, when kept at an ambient temperature of 25°C. Adapted from "Quantifying the instability of core temperature in rodents" by C. J. Gordon, 2009. Journal of Thermal Biology, 34, 213-219.

In addition to the fluctuations in metabolic rate caused by circadian rhythm, there are also general differences between male and female metabolic rates. Females tend to have a higher body temperature, higher resting metabolic rate, and larger levels of BAT (Lynch et al., 1976). Females also have a higher threshold temperature (~22°C) for thermogenic response than males do (~18°C). This is indicated by experiments showing that female rodents express higher levels of UCP-1 in BAT at 22°C compared to males, indicating a cold-induced thermogenic response in females but not males at this temperature. This is supported by behavioural experiments showing that when given a

choice, female mice usually prefer higher ambient temperatures than male mice (Kaikaew et al., 2017). This may be due to the fact that females tend to be smaller than males, meaning they lose more heat to their environment because of their higher surface area to volume ratio (Gaskill et al., 2008). However, in cold environments (4°C), male and female rodents show similar levels of UCP-1 (Quevedo et al., 1998).

1.3 Thermosensing mechanisms

As a vital mechanism for survival, scientists have spent decades researching how the precise and dynamic thermoregulatory responses are generated and maintained. A mammal senses temperature changes through cutaneous thermoreceptors which are relayed to the brain via ascending projections (Bratincsak and Palkovits, 2005). The transient receptor potential (TRP) cation channels have been identified as the thermoreceptors responsible for initiating thermoregulatory responses.

There are various channels in the TRP: Melastatin (TRPM), Ankyrin (TRPA), and Vanilloid (TRPV) families that are activated by both cold and hot sensation. TRPV1-4 are heat-activated channels that each respond to a specific range of temperatures across a gradient from warm to noxious heat (27- 52°C). The cold-activated channels TRPM8 and TRPA1 aid in the perception of innocuous cool (15-30°C) to noxious cold temperatures (below 15°C) (Dhaka et al., 2006). Animals lacking the TRPM8 channel ($TRPM8^{-/-}$) show impairments in sensing and discriminating between cool and noxious cold temperature, but the ability to sense warm and noxious hot temperatures was maintained. Contrastingly, TRPA1 deficient mice do not show deficits in responding to cold temperatures. Therefore, TRPM8 has been identified as the primary detector of environmental cold (Bautista et al., 2007).

While the majority of TRPM8 expression is seen in peripheral nerve endings and the primary sensory neurons that they project to, there are also lower levels of TRPM8-expressing neurons in the rodent brain. TRPM8 expression has been identified in areas relating to autonomic thermoregulation, including the preoptic area of the hypothalamus (POA) (Ordas et al., 2019).

1.4 Thermoregulatory brain regions

The POA was discovered as the brain centre responsible for initiating behavioural and autonomic responses to combat environmental temperature change (Hammel, 1968). It was later found that peripheral skin warming leads to an increased firing rate in specific neurons, named warm-sensitive neurons (WSN), in the POA, a portion of which are also responsive to local hypothalamic temperature changes (Boulant and Hardy, 1974, Boulant and Bignall, 1973). Neurons that increase their activity in response to ambient or local cooling, called cold-sensitive neurons (CSN), were also found in the POA (Hori, 1991).

The POA of the hypothalamus encompasses areas and nuclei that are involved in specific thermoregulation processes. One such area, the median preoptic nucleus (MnPO), plays a vital role in initiating shivering, vasoconstriction in the periphery, and BAT thermogenesis. The MnPO was first identified as a critical area in thermoregulatory response through c-Fos immunohistochemistry, which is a method used to visualise recently active neurons. This technique takes advantage of the proto-oncogene *c-fos*, which is an immediate early gene (IEG) expressed in many neurons after depolarisation. The protein product c-Fos is subsequently expressed in these neurons and can be identified using immunohistochemistry as a marker of recent neuronal activity (Bullitt, 1990). Using this method, researchers were able to pinpoint the various regions within the brain that are activated after recent ambient cold or warm exposure (Bratincsak and Palkovits, 2004). The MnPO of rats was identified as having moderate to high levels of c-Fos expression in response to ambient cold and warmth (Bratincsak and Palkovits, 2004).

After locating both WSN and CSNs in the POA and various other brain regions, it was hypothesised that WSNs were responsible for activation of behavioural and autonomic responses promoting heat loss, while CSNs were in control of heat production. However, it has since been shown that autonomic responses promoting heat production, including shivering, skin vasoconstriction and non-shivering thermogenesis, are actually predominantly controlled by WSNs with much less contribution from CSNs (Zhang et al., 1995, Chen et al., 1998). Glutamatergic stimulation of MnPO neurons leads to an increase in cold-defensive responses, such as increased sympathetic nervous

activity to BAT and increased metabolic rate, while inhibition of MnPO neurons with glycine blocks these responses (Nakamura and Morrison, 2008).

1.4.1 Brain circuits driving thermoregulation

The circuits for sensing and reacting to environmental warm and cold exposure have since then been further elucidated. In a recent review, Nakamura and Morrison clearly outline the individual pathways for cold-sensing and warm-sensing (Figure 1.4.1)(Morrison and Nakamura, 2019). Both pathways begin with thermoreceptors in the skin relaying afferent signals to unique populations of neurons in the dorsal horn (DH) of the spinal cord, then on to different neuronal populations in the lateral parabrachial nucleus (LPB), which is located between the medulla and the pons. The sensory signals are then relayed to the POA in the hypothalamus, which integrates the information from cutaneous thermoreceptors with feedback about the core temperature of internal organs and information from the pyrogenic mediator PGE_2 signifying infection or inflammation (Morrison and Nakamura, 2019).

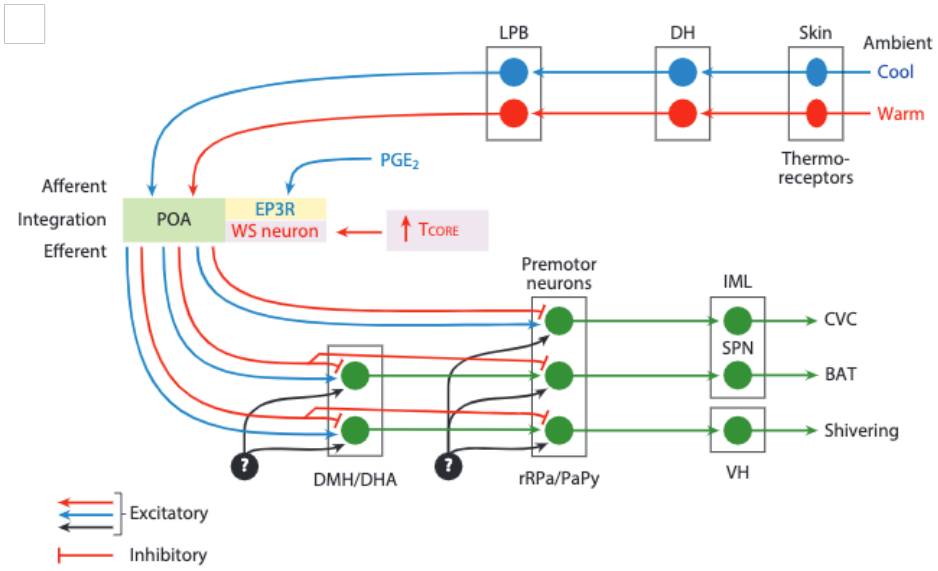

Figure 1.4.1: Schematic showing the neural circuits for thermoregulatory responses. Blue and red pathways represent autonomic responses to ambient cool and warmth, respectively. Green lines show efferent pathways regulated by inputs from the POA, which are either inhibitory (red) or excitatory (blue). Black arrows represent tonic excitatory inputs to the DMH/DMA and rRPA with unknown sources. Adapted from "Central Mechanisms for Thermoregulation" by S.F. Morrison and K. Nakamura, 2019. Annual Review of Physiology, 81:285–308.

Until this point, the afferent signals for warm sensing and cold sensing follow the same excitatory pathway, although they excite different neuronal populations within the

various relay centres. However, from the POA, the efferent signals from the ambient warm pathway have an inhibitory effect on the downstream areas, whereas the efferent signals from the ambient cold pathway continue to exert an excitatory effect on the downstream areas. Leaving the POA, the inhibitory warm and excitatory cold efferent signals travel to the premotor neurons in the rostral raphe pallidus nucleus (rRPa) and the parapyramidal area in the medulla (PaPy) either directly or via the dorsal hypothalamic area/nucleus (DHA/DMH). Finally the efferent signals travel back to the spinal cord to initiate autonomic cold-defensive responses. Shivering thermogenesis is initiated by the ventral horn (VH), whereas BAT thermogenesis and cutaneous vasoconstriction are controlled via the sympathetic preganglionic neuron (SPN) and the intermediolateral nucleus (IML) of the spinal cord, respectively.

While this pathway outlines the autonomic responses to ambient warm and cold exposure, it does not address the behavioural responses. It has been shown that various regions in the hypothalamus, including the POA, the DMH, and the posterior hypothalamus are involved in behavioural responses to temperature change, such as saliva spreading to induce evaporative heat loss, and warmth or cold-seeking/avoidance (Almeida et al., 2015). However, the exact circuits responsible for these behaviours have yet to be elucidated (Morrison and Nakamura, 2019).

1.4.2 Functional experiments testing thermoregulatory brain circuits

Most of the experiments to define thermoregulatory circuits have utilised electrophysiology, retrograde tracing, and immunohistochemistry. The application of optogenetic approaches have allowed more specificity and interrogation of the characteristic and function of precise populations of neurons. Optogenetics allows for the genetic labelling of specific cells with opsins that can be activated by a specific wavelength of light administered through an implanted fibre optic cannula in alive behaving rodents (Aravanis et al., 2007, Fenno et al., 2011). Through the injection of viral vectors into the brain, or transgenic opsin-expressing rodent lines, the opsins can be targeted to regions of interest and even to specific cell-types. Labelled neurons can then be activated by light *in vivo* (Aravanis et al., 2007, Fenno et al., 2011).

To better define the characteristics and function of the neurons in the heat-defensive circuit, researchers used immunohistochemistry to identify neurons in the ventral part of the lateral preoptic nucleus (vLPO) that were active in response to heat. These neurons also co-localised with GAD67, a GABAergic marker, suggesting that the heat-activated neurons are GABAergic in nature. Cre-dependent adeno-associated viruses (AAV) were injected into the vLPO of Vgat-IRES-Cre driver mice to label all the GABAergic neurons in the vLPO with Channelrhodopsin-2 (ChR2) fused to Enhanced Yellow Fluorescent Protein (EYFP). Subsequent activation of labelled neurons using blue light invoked heat-defensive behaviours, including reduced core temperature and decreased activity. To optogenetically inhibit neurons, Guillardia theta anion channelrhodopsin 1 (hGtACR1) was used to silence neuronal activity in response to blue-yellow light (Govorunova et al., 2015). Optogenetic inhibition of hGtACR1-expressing neurons in the vLPO led to the reciprocal thermoregulatory behaviour, hyperthermia (Zhao et al., 2017).

Other researchers have identified neurons in a neighbouring region, the ventromedial preoptic area (VMPO) that were active in response to a warm-challenge. RNA sequencing revealed that the expression of specific genes could be used to identify warm-activated neurons. The expression of neuropeptides pituitary adenylate cyclase-activating polypeptide (PACAP) and brain-derived neurotrophic factor (BDNF) in warm-activated cells did not overlap with the neurons activated in cold challenge. Cre and LacZ transgenic mouse strains were used to localise neurons that expressed both PACAP and BDNF. Injecting Cre-dependent AAVs into the VMPO targeted expression of a stabilised step function opsin (SSFO) to VMPO$^{PACAP/BDNF}$ neurons and allowed for light-induced activation of the neurons *in vivo* (Tan and Knight, 2018). Stimulation of the VMPO$^{PACAP/BDNF}$ neurons induced hypothermia in the mice, characterised by an increase in tail vasodilation and a decrease in BAT temperature. These findings suggest that activating VMPO$^{PACAP/BDNF}$ neurons results in an increase in heat dissipation strategies and an inhibition of heat producing responses. When placed on a thermal gradient while simultaneously activating VMPO$^{PACAP/BDNF}$ neurons, mice moved towards the colder portion of the gradient, indicating that these neurons are important for behavioural responses as well as autonomic responses. Activation of VMPO$^{PACAP/BDNF}$ neurons also blocked cold-defensive behaviours (such as nest

building and seeking warmer temperatures on the thermal gradient) even in the presence of the super-cooling agent icilin (Tan and Knight, 2018).

These elegant experiments utilising genetic promoters to label temperature-activated neurons provide information about the function and characteristics of specific neuronal populations, however they lack temporal specificity. In order to better understand many of the unanswered questions in the thermoregulation field, it would be advantageous to optimise a technique to label the specific neurons activated during temperature exposure. To do this, we can draw on novel engram labelling techniques used in memory research.

1.5 Engram labelling

Engram labelling strategies combine optogenetics with transgenic labelling, resulting in the ability to tag and manipulate a specific population of neurons after they have been active *in vivo*. When the IEG promoter is coupled with a temporally inducible transactivator, it provides a designated time window in which active cells will be tagged. The IEGs used to label neurons are fused to opsins, such as Channelrhodopsin-2 (ChR2), which can be activated by specific wavelengths of light. When artificial light is targeted to these neurons (usually through optogenetic fibres implanted above the region of interest) it results in the activation of the labelled neurons in awake behaving rodents (Liu et al., 2012).

For example, one strategy utilises a c-fos-tTA transgenic mouse, in which a *c-fos* promoter drives expression of the doxycycline(Dox)-dependent tetracycline transactivator (tTA). When Dox is not present, tTA binds to tetracycline-responsive element (TRE) and drives expression of ChR2, which is usually fused to enhanced yellow fluorescent protein (EYFP). Introducing Dox inhibits tTA from binding to TRE, which prevents neurons from being tagged with ChR2-EYFP. However, when Dox is removed for a specific time window, the recently active neurons expressing *c-fos* will be labelled with ChR2-EYFP, resulting in activity and time dependent labelling (Ryan et al., 2015).

Another strategy, based on iCre recombination, involves crossing two transgenic mouse lines to create a FosTRAPxAi32 line. The FosTRAP transgenic line expresses the *c-fos* promoter under the control of 4-hydroxytamoxifen (4-OHT). The Ai32 line expresses ChR2-EYFP in response to Cre recombinase. Therefore, in the presence of 4-OHT, the *c-fos* promoter drives Cre recombinase at the loxP sites, resulting in removal of the stop codon and expression of ChR2-EYFP driven by the pCAG promoter (Madisen et al., 2012).

Using engram technology, researchers have identified ensembles of neurons that are active during encoding a memory and are also necessary and sufficient to recall said memory (Liu et al., 2012, Tanaka et al., 2014). Through this approach, researchers have also shown that memories can be altered through the activation and pairing of different neuronal ensembles during learning and recall (Liu et al., 2014). These findings and many others have greatly advanced our understanding of learning and memory, however there is far less known about the mechanisms driving instinctual responses. The application of engram technology to instinct research would provide the opportunity to investigate many unanswered questions. As an innate response, temperature regulation provides a platform through which we can investigate these questions.

1.6 Role of memory in thermoregulation

Not only would the application of engram-technology be advantageous to understanding the basic mechanisms driving innate responses, but it would also provide invaluable information about the potential for shared encoding mechanisms between learned and instinctual responses. It has been hypothesised that memories and instincts are coded in the brain in the same way (Ryan, 2020). Instincts are the innately encoded responses that organisms have developed in response to their environments (Tinbergen, 1951). On the other hand, memories are learned behaviours which sometimes build upon instincts. The knowledge that these two types of information can interact warrants the question of whether they are dependent on similar neuronal processes.

Building on the hypothesis that memories and instincts are encoded in a similar way, it begs the question of whether innate information is included in memories and vice versa.

It would be advantageous for a mammal to remember areas in which they have had extreme temperature experiences. Then, if these places were ever encountered again, the mammal could anticipate the temperature and begin to immediately respond in a way that would be most efficient to defend the core body temperature.

There is evidence that animals learn to associate temperature with specific contexts. In Pavlovian fear conditioning experiments, rats are placed in a unique context and given an aversive stimulus, such as a foot shock (unconditioned stimulus (US)), which elicits an unconditioned fear response, such as freezing behaviour. After one or more training sessions, rats learn to associate the context, or conditioned stimulus (CS), with the foot shocks and elicit freezing behaviour, conditioned responses (CR), to the context alone. Rats also show an increase in core body temperature in response to the shock-paired context. This indicates that core body temperature can be used as a CR in Pavlovian fear conditioning experiments (Godsil et al., 2000, Vianna and Carrive, 2005). However, it also indicates that memory might play a role in thermoregulatory mechanisms. If temperature information can be associated with a context then it is possible that memory is able to alter innate responses. This research project aims to understand whether innate behavioural and physiological temperature responses can be altered through learning.

1.7 Aims and Objectives

The thermoregulatory field has made phenomenal progress in the recent decades, however there is still a lot to be learned about the basic mechanisms of autonomic and behavioural responses to temperature challenge. This research project will specifically focus on the role of learning and memory in thermoregulatory responses. To investigate these factors, engram labelling technology will be employed to label and manipulate the exact neuronal population active during a temperature exposure. These tools will allow for investigation into whether thermoregulatory responses can be modulated by learning. Thermoregulatory responses could be hard-wired without any margin for change, or they could be malleable with the potential for re-wiring based on learning. Understanding the way innate responses are stored in the brain would also shed light on whether there is a thermoregulatory component encoded as part of memory engrams.

Investigating the relationship between thermoregulatory responses and contextual memories would also provide a means for understanding the way in which instincts are encoded in the brain. By uncovering the mechanisms responsible for thermoregulatory responses, we could test the hypothesis that memories can alter innate responses.

Chapter 2: Materials and Methods

2.1 Subjects and engram labelling strategy

2.1.1 Subjects

All experiments were conducted in accordance with the Health Products Regulatory Authority (HPRA) Ireland guidelines. C57BL6/J and fosTRAPxAi32 mice were used for these experiments. The fosTRAPxAi32 mouse line was created by breeding Fos-iCre mice with Ai32(RCL-ChR2(H134R)/EYFP) mice and experimental animals were limited to offspring carrying both the CreERT and EYFP transgenes (Allen et al., 2017, Madisen et al., 2012). Adult (7-17 week old) male and female mice were used. Mice were group housed by sex with access to food and water *ad libitum*. Animals were bred in house at Trinity Biomedical Sciences Institute and were kept at a constant temperature of 22°C and a 12 hour night/dark cycle. All experiments except the night time experiment were conducted during the light cycle.

2.1.2 Engram Labelling Strategy

The tTA labelling strategy was used for tagging temperature-sensitive neurons *in vivo*. C57BL6/J mice were placed on a doxycycline diet (Datesand Group) 24 hours before stereotactic surgery and remained on the diet until the labelling phase. During surgery, mice were injected with a 1:5 dilution of AAV9-cfos-tTA (Vigene Biosciences) and 4:5 dilution of AAV9-TRE-ChR2-EYFP (Vigene Biosciences). The doxycycline diet was removed 36 hours pre-exposure to the labelling environment. After the 4-hour temperature exposure during which the temperature-sensitive neurons were labelled, mice were placed back on a doxycycline diet for the remainder of the experiment.

The Cre labelling strategy was also used for tagging temperature-sensitive neurons *in vivo*. FosTRAPxAi32 transgenic mice were placed in the training context for a 4-hour temperature exposure. Immediately after the exposure, the mice were injected intraperitoneally with 4-OHT to activate iCre recombinase. The iCre recombinase acts on loxP sites in the nucleus to remove a stop codon and thus allow for expression of the ChR2-EYFP transgene driven by the pCAG promoter. All iCre expressing neurons

active during temperature exposure will then express ChR2-EYFP after 72 hours. For double injection, 4-OHT was injected immediately after exposure and 2 hours post-exposure.

2.1.3 Stereotactic surgery

All surgeries were performed using a digital stereotaxic frame (WPI). Mice were anaesthetised with 500 mg kg^{-1} avertin and head fixed on the setup. For analgesia, Meloxicam (0.075 mL/5g) was given via a subcutaneous injection, EMLA cream was administered to the ear canals, and lidocaine was provided locally to the scalp via a subcutaneous injection. Ophthalmic ointment (vidisic gel) was applied to the eyes to prevent drying. The incision site was cleaned with chlorhexidine before opening the skin at the midline of the scalp. Ethanol and PBS were used to clean the skull and bregma was identified. One hole was drilled at +0.3mm anteroposterior (AP), 0.0mm mediolateral (ML) coordinates for the injection site. A micro syringe pump (UMP3;WPI) and a 10 µL Hamilton syringe (701LT; Hamilton) were used to inject 500nl of the AAV cocktail at +0.3mm (AP); 0mm (ML); -4.75mm dorsoventral (DV). After the needle was introduced into the brain it was left at the location for 5 minutes before the injection was given. After the injection, the needle remained in the same place for 10 minutes. After the needle was removed, the skin was sutured over the incision site and mice were left in a warm box (29°C) to recover from anaesthesia. For 2 days following surgery, mice were given an intraperitoneal injection of meloxicam once a day. Mice were allowed to recover for 2 weeks post-surgery before the behavioural part of the experiment commenced.

2.2 Immunohistochemistry

2.2.1 Brain slice preparation

Mice were sacrificed via an overdose injection of Sodium Pentobarbital (50 µL) followed by transcardial perfusion with PBS and then 4% paraformaldehyde (PFA) in PBS. Brains were dissected from the skull and kept in 4% PFA at room temperature overnight. After 24 hours, brains were moved to PBS and stored at 4°C. Brains were sectioned coronally into 50 µm slices using a vibratome.

2.2.2 Immunostaining

Slices were washed 3 times for 10 minutes with PBS + 0.2 % Triton X-100 (PBS-T). Following this, slices were incubated with PBS-T 0.2% + 10% normal goat serum (NGS) for 1 hour at room temperature. Slices were then incubated for 24 hours at 4°C with primary antibody. Following this, slices were washed 3 times for 10 minutes in PBS-T 0.2%. Slices were then incubated for 2 hours at room temperature in secondary antibody. Slices were then washed 2 times for 10 minutes in PBS-T 0.2% followed by 1 wash for 10 minutes in DAPI+PBS. Slices were then mounted on Superfrost slides with Vectashield-DAPI (Vector Labs).

For ChR2-EYFP staining, the primary antibody used was chicken anti-GFP IgY fraction (Invitrogen) (1:1000) and visualised using secondary antibody anti-chicken Alexa-488 IgG (H+L) (Invitrogen) (1:500). c-Fos was stained with rabbit anti-c-Fos (Synaptic Systems) (1:500) and anti-rabbit Alexa-568 (Invitrogen) (1:500).

2.2.3 Image Acquisition

An Olympus Bx51 fluorescence microscope was used for imaging the samples. Images were taken with a magnification of 4x, 10x, or 20x. The MnPO was identified in slices ranging from Bregma 0.62mm-0.245mm (anterior to posterior). Single pane images of the MnPO were taken every 0.1mm throughout this area.

2.2.4 Cell Counting

Single pane images from the Allen Adult Mouse Brain Atlas were used as a reference to create templates for the MnPO region, spanning from Bregma 0.62mm-0.245mm (AP), taken every 0.1mm (Lein et al., 2007). Using Adobe Photoshop CC 2018 software, the Allen Adult Mouse Brain Atlas templates were overlaid on each single pane microscope image of the corresponding AP coordinate and the cells stained for c-Fos within the selected region were counted on both hemispheres. Cell counting was performed blind to the experimental conditions.

2.3 Behavioural protocols and metabolic measurements

2.3.1 Metabolic cages

Promethion temperature controlled metabolic cages (Sables Systems International) were used for temperature training and data acquisition. Metabolic cages were calibrated before each run. During the run, mice were individually housed in identical cages within the temperature controlled cabinet. EE was calculated using the Weir equation (Weir, 1949). CO_2 was measured through indirect calorimetry parameters specified by the Promethion system. Metascreen software was used for data acquisition and Sable Systems Macro Interpreter software was used to export the data. The first hour of each recording was excluded due to calibration inconsistencies. Exported data was uploaded to CalR for statistical analysis using the Two group acute response template (Mina et al., 2018).

2.3.2 Anticipatory cold-context association protocol

Mice were weighed each day prior to being placed in the metabolic cages. On the first day (Baseline 1), mice were placed in Context A and the temperature remained at 21°C throughout the exposure. On days 2-4 (Cold days 1-3) mice were placed in Context B with the temperature beginning at 21°C and then ramping down to 4°C for the remainder of the exposure. On day 5 (Baseline 2) mice were placed in Context A and the temperature remained at 21°C throughout the exposure. On day 6 (Test) mice were placed in Context B and the temperature remained at 21°C throughout the exposure.

Context A conditions included striped wall pattern, acetic acid (1% in H_2O) odorant, normal home cage bedding, 100% light, and 100% fan. Context B conditions included circle wall pattern, benzaldehyde (0.25% in EtOH) odorant, white paper floor, 50% light, and 50% fan.

For the 16 hour post-exposure experiments, the Baseline 2 day was not included and instead the Test day followed directly after the Cold day 3. For day time experiments, mice were placed in the metabolic cages at ~10:00 and removed at ~18:00. The 8 hour exposure consisted of 2 hours temperature ramp followed by 6 hours temperature exposure. For night time experiments, mice were placed in the metabolic cages at

~22:00 and removed at ~08:00. The 10 hour exposure consisted of 2 hours wait, followed by 2 hours temperature ramp, and then 6 hours temperature exposure.

2.4 Tissue dissection and analysis

2.4.1 Tissue dissection

Immediately after mice were removed from the metabolic cages on Test day, they were sacrificed using Carbon Dioxide overdose. Ethanol was used to clean the incision site and then the interscapular skin was removed. The interscapular brown adipose tissues (iBAT) was dissected and placed in a CryoTube which was then submerged in liquid nitrogen. Samples were stored at -80°C.

2.4.2 RNA extraction and RT qPCR

iBAT was homogenised using tissue lyser II (Qiagen) for 2 minutes at 25/s frequency. RNA was extracted using TRIzol reagent (Invitrogen) and following instructions from the manufacturer. Quantiscript reverse transcriptase enzyme (Qiagen) was used to copy 2000ng of RNA to cDNA for a final volume of 20 µl. Real-time PCR was performed in QuantStudio3 (Applied Biosystems) using iTaq Universal SYBR® Green Supermix (Bio-Rad). Thermocycler conditions recommended by the manufacturer were used. PCRs were conducted in duplicates in a total volume of 20 µl containing 0.5 µl of the reverse transcription reaction. The average cycle threshold (CT) of the UCP-1 gene for each sample was normalised against the PPIB housekeeping gene to get the δCT. The average δCT values for the male daytime group was used as the control group and other groups were normalised against this using the δδCT method.

2.5 Statistics

GraphPad Prism 6.00 software was used for data analysis and statistics. Weight and UCP-1 fold change comparisons between 2 groups were calculated using unpaired Student's t-tests. EE values from anticipatory cold-context association protocol were compared using paired Student's t-tests. c-Fos+ cells were compared between 3 groups using one-way ANOVA. Repeated measures Two-way ANOVA analysis was used to compare EE and CO_2 data from the cold-text association protocols.

Chapter 3: Results

3.1 Identifying neurons activated in the MnPO by ambient cooling and warming

The first aim of this project was to identify temperature-sensitive neurons in the MnPO region of the hypothalamus. To do so, mice were placed in a temperature controlled cage for 4 hours at either hot (37°C), cold (4°C), or thermoneutral (29°C) conditions. The level of c-Fos expression in the MnPO was then quantified and compared between the groups (Figure 3.1.1).

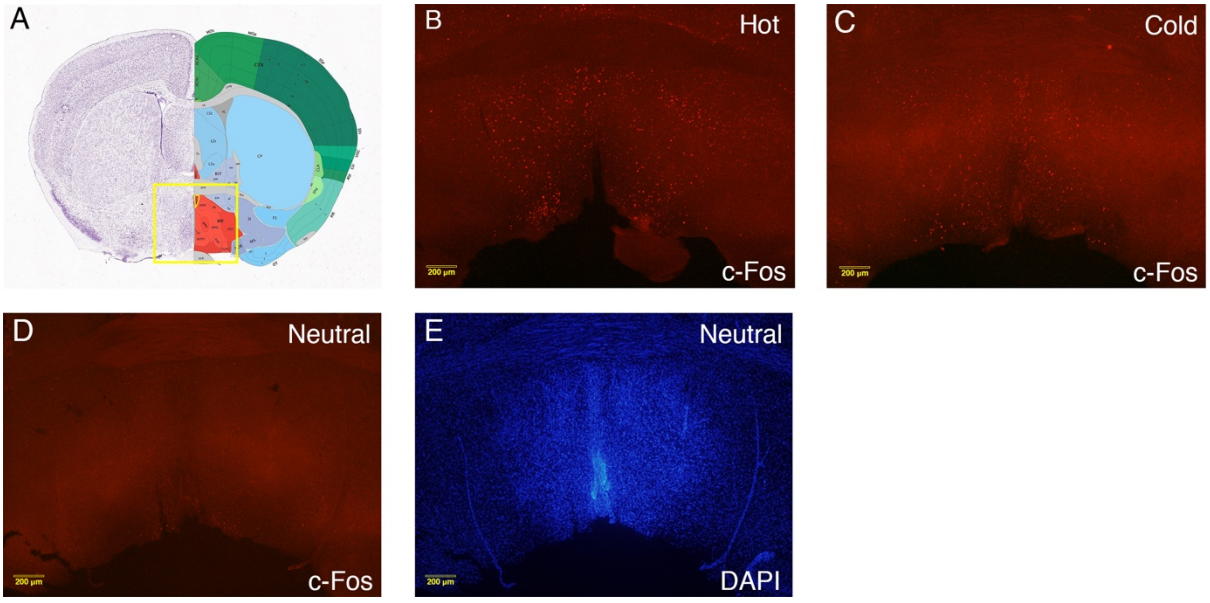

Figure 3.1.1 A. Image showing a coronal section at level 53 (Bregma 0.145) from an adult mouse brain with Nissl staining on the right hemisphere and atlas image on the left hemisphere. Areas of the hypothalamus are highlighted in red on the left hemisphere. The MnPO region is outlined in yellow, ventral of the anterior commissure. The yellow box shows the area represented in the following 3 microscope images. Image taken from Allen Adult Mouse Brain Atlas (Lein et al., 2007). **B.** Representative image of c-Fos staining in mouse brain slice taken after 4 hours at 37°C (4x magnification; scale: 200 µm). **C.** Representative image of c-Fos staining in mouse brain slice taken after 4 hours at 4°C (4x magnification; scale: 200 µm). **D.** Representative image of c-Fos staining in mouse brain slice taken after 4 hours at 29°C (4x magnification; scale: 200 µm). **E**. Representative image of DAPI staining in mouse brain slice taken after 4 hours at 29°C (4x magnification; scale: 200 µm).

The group of mice exposed to hot conditions showed significantly higher c-Fos expression than the group exposed to thermoneutrality (Figure 3.1.2). These results corroborate with previous findings indicating that there are more warm-activated neurons than cold-activated neurons in the POA (Zhang et al., 1995, Hori, 1991).

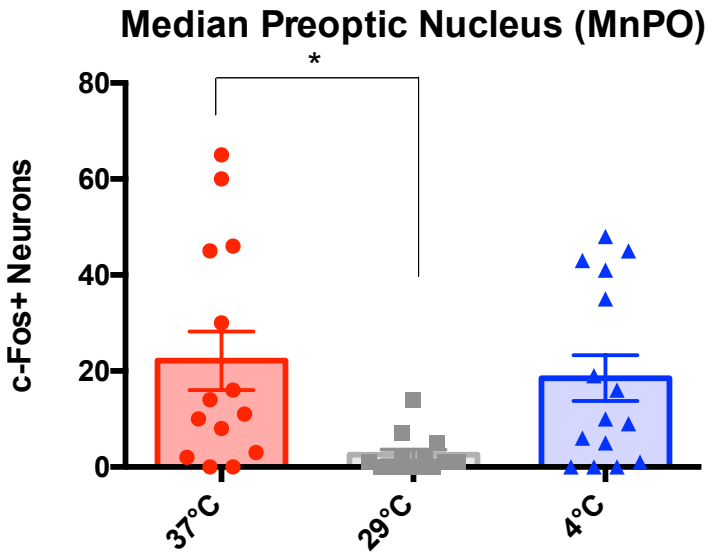

Figure 3.1.2: Comparison of c-Fos+ neurons at 3 different temperatures, 37°C (n=4), 29°C (n=4), 4°C (n=4). Multiple brain slices taken from the MnPO (anterior-posterior: Bregma 0.62-0.245mm) of the same animal were used for c-Fos counts. The group exposed to 37°C showed significantly higher c-Fos+ neurons compared to the group exposed to 29°C. Statistical comparisons performed using one-way ANOVA with Bonferroni's multiple comparison test (p=0.0132). Error bars show mean ± S.E.M. Two outliers detected using Grubbs' Test Alpha (0.05) and removed before analysis.

3.2 Labelling neurons in the POA using engram technology

3.2.1 tTA Labelling Strategy

After identifying neurons in the MnPO using c-Fos IHC, the next aim was to label and manipulate the hot, cold, and neutral responding neurons within this region. The tTA engram labelling strategy was used, which involves stereotactic injection of a cfos-tTA and TRE-ChR2-EYFP AAV cocktail into the MnPO region. Following this, bilateral cannulas were implanted above the injection site. Mice were kept on a doxycycline diet before and after surgery to prevent labelling. The diet was removed 36 hours before the temperature exposure to open the window for labelling of active neurons during the experience. Then, mice were exposed to either hot (37°C), cold (4°C), or neutral (29°C) temperatures for 4 hours while in Sable Systems Promethion metabolic cages to measure the physiological responses of the mice during temperature exposure. After the labelling, mice were put in a different context and the labelled neurons were optogenetically stimulated.

Post-mortem analysis showed that the labelling of temperature-sensitive neurons in the MnPO was unsuccessful. There were neurons labelled in the MnPO in 3 out of 12 experimental mice, with 1 in the 4°C group and 2 in the 29°C group (figure 3.2.1).

There was strong labelling in peripheral regions (figure 3.2.1C, F) but much weaker labelling in the MnPO. The experiment was repeated and in total, less than 30% of experimental mice showed labelling, which was not a high enough percentage to justify continuing with this method. We hypothesised that the inability to label the MnPO neurons was potentially due to cell death caused by the c-fos tTA virus overexpressing. In previous applications of the tTA labelling strategy, the duration of the labelling period is usually around 15 minutes. The protocol used in this experiment included a labelling period that was 4 hours in duration. Additionally, the hot and cold temperatures used for the labelling period were extreme stimuli that we anticipated would produce a large response from neurons in the MnPO region. Therefore, we hypothesised that the prolonged and intense temperature exposure during the labelling period caused overexpression of the c-fos tTA virus that led to cell death in this region, and resulted in unsuccessful labelling of active neurons in the MnPO. This hypothesis is corroborated by the evidence showing stronger labelling in the peripheral regions of the hypothalamus, where there might not have been as much tTA virus expression, and therefore less cell death than in the MnPO.

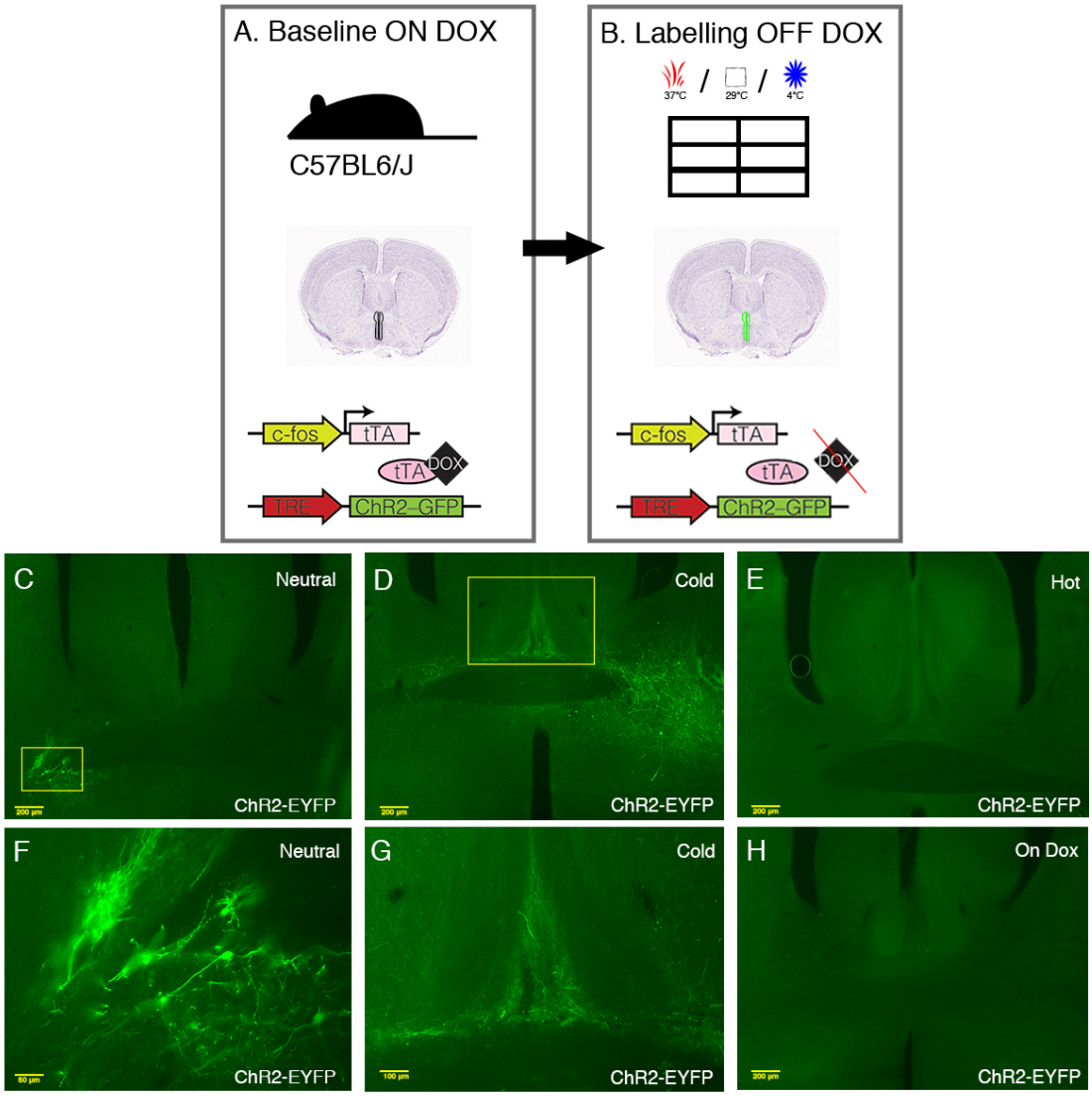

Figure 3.2.1: A. Schematic depiction of the tTA labelling method. AAV injection was targeted to the MnPO, which is the long narrow structure that is outlined at the midline. C57BL6/J mice were kept on a doxycycline diet (ON DOX) before and after surgery, which prevents the tTA trans-activator from binding the TRE promoter. **B.** When the doxycycline diet is removed (OFF DOX) the tTA transactivator binds to the TRE promoter, resulting in the expression of ChR2 in recently active cells in the targeted region (MnPO) during exposure to 37°C, 4°C, or 29°C. **C.** Representative images from 29°C group (n=4) of ChR2-EYFP labelling (bright green) seen in peripheral regions but not in the MnPO (4x magnification; scale: 200 µm). Yellow box represents insert which is shown in F. **D.** Representative images from 4°C group (n=4) of ChR2-EYFP labelling (bright green) in the MnPO (4x magnification; scale: 200 µm). Yellow box represents insert which is shown in G. **E.** Representative image from 37°C group (n=4) which did not show ChR2-EYFP labelling (4x magnification; scale: 200 µm). **F.** ChR2-EYFP labelling (bright green) in peripheral region of brain slice taken from 29°C group (n=4) (20x magnification; scale; 50 µm). **G.** ChR2-EYFP labelling (bright green) in the MnPO in brain slice taken from 4°C group (n=4) (10x magnification; scale: 100 µm). **H.** Representative image from control group that was kept on a doxycycline diet throughout the experiment (n=4). No ChR2-EYFP labelling was detected in this group (4x magnification; scale: 200 µm).

However, the metabolic data collected during temperature exposures showed a number of differences in behavioural and physiological responses between the 4°C, 29°C, and

37°C groups. The strongest effect was seen in EE, with the cold (4°C) group showing significantly higher EE than the thermoneutral (29°C) group (Figure 3.2.2). The hot (37°C) group also showed significantly higher EE than the neutral group, but the effect was not as profound.

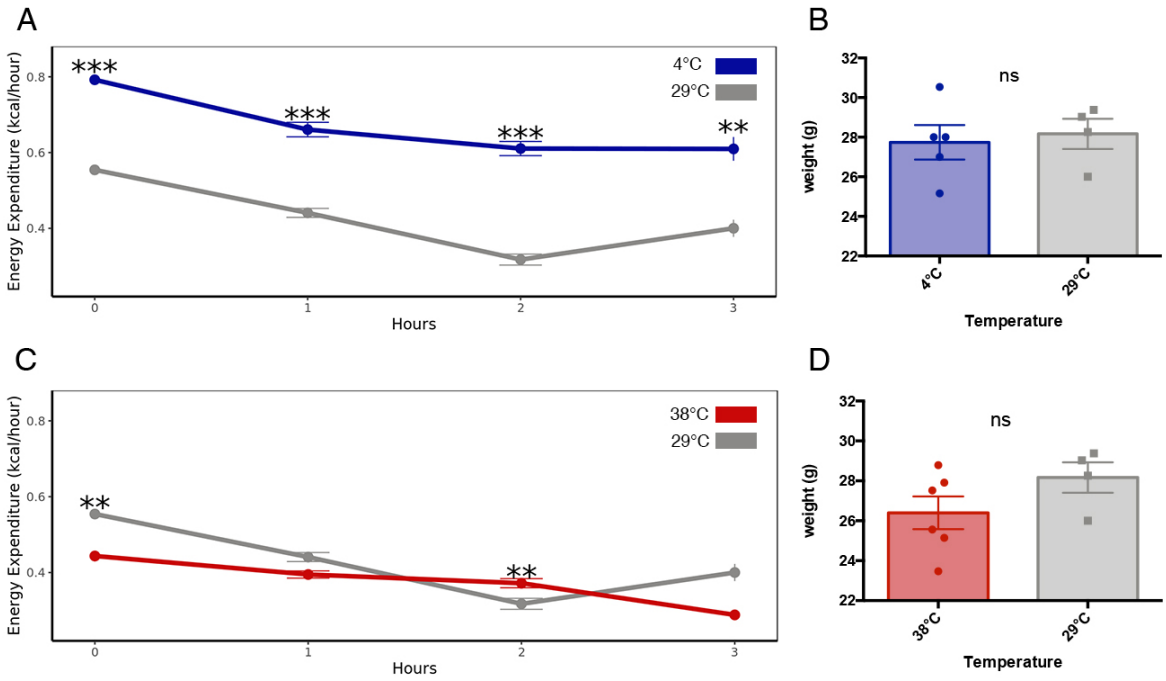

Figure 3.2.2: A. The 4°C (n=6) group showed significantly higher EE compared to the 29°C (n=4) throughout the exposure. Statistical analysis was done using CalR, with GLM analysis showing significance levels of p<0.001 (***) for hour 0, 1, and 2 timepoints and p=0.0042 (**) for hour 3 timepoint. Error bars represent S.E.M**. B.** The weights of the 4°C and 29°C groups range from 25-30g. The weight of one animal was measured incorrectly by the software and thus was removed from analysis. A two-tailed unpaired t-test showed there was no significant difference between the weights of the two groups (p=0.7224). **C.** The 29°C group (n=4) showed a significantly higher EE than the 37°C group (n=6) at hour 0 (p=0.0049), whereas the opposite effect occurred at hour 2 (p=0.0033). **D.** The weights of the 37°C and 29°C groups range from 23-29g. A two-tailed unpaired t-test showed there was no significant difference between the weights of the two groups (p=0.1533). Significance denoted in A-D as: ns p>0.05, * p≤ 0.05, ** p≤ 0.01, *** p≤ 0.001, **** p≤ 0.0001. Error bars show mean ± S.E.M.

3.2.3 Cre Labelling Strategy

Since the tTA labelling strategy was unsuccessful for reliably labelling MnPO neurons, we also tried a CRE-based engram labelling technique. FosTRAPxAi32 transgenic mice were exposed to hot (37°C), neutral (29°C), or cold (4°C) temperatures for 4 hours while in Sable Systems Promethion metabolic cages. Immediately after the temperature exposure, mice were injected intraperitoneally with 4-OHT to label the neurons that had

been active during the temperature exposure. Post-mortem analysis revealed successful labelling of some neurons in the MnPO (Figure 3.2.3).

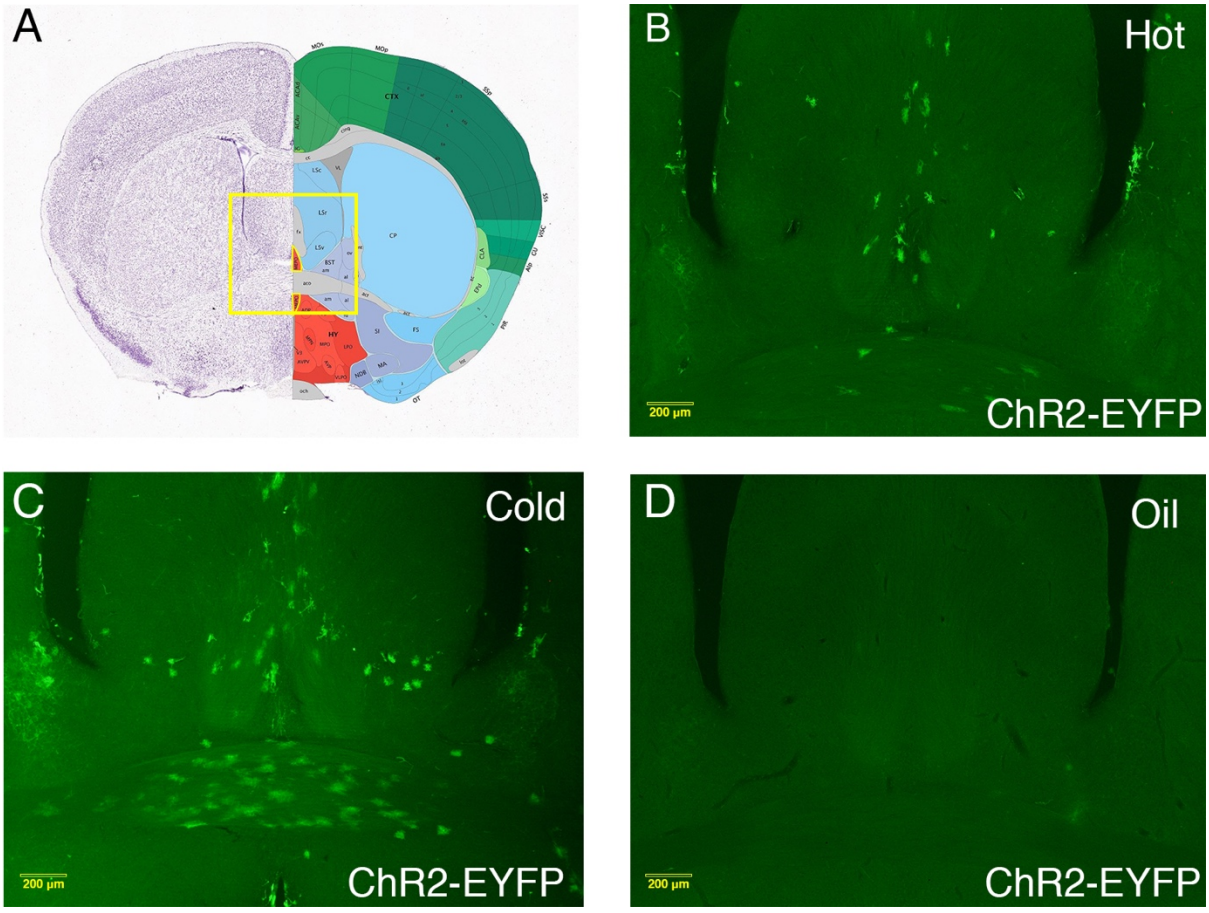

Figure 3.2.3: A. Image showing a coronal section at level 53 (Bregma 0.145) from an adult mouse brain with Nissl staining on the right hemisphere and atlas image on the left hemisphere. Areas of the hypothalamus are highlighted in red on the left hemisphere. The MnPO region is outlined in yellow, ventral and dorsal of the anterior commissure. The yellow box shows the area represented in the following 3 microscope images. Image taken from Allen Adult Mouse Brain Atlas (Lein et al., 2007). **B.** Representative images from 37°C group (n=2) of ChR2-EYFP labelling (bright green) at 4x magnification (scale: 200 µm). **C.** Representative images from 4°C group (n=5) of ChR2-EYFP labelling (bright green) at 4x magnification (scale: 200 µm). **D.** Representative images from control group (n=3) that was exposed to 29°C and received an oil injection instead of 4-OHT (4x magnification scale: 200 µm). No ChR2-EYFP labelling was detected in this group.

Our results showed a very small number of temperature-sensitive neurons labelled in the MnPO and therefore we wanted to optimise this aspect. There is evidence that a double injection of 4-OHT after stimulus exposure is more effective at labelling neurons in adult mice (Power, S. unpublished). Therefore, we adopted this strategy and saw a higher number of labelled neurons in animals that received a double injection of 4-OHT compared to single injection (Figure 3.2.4).

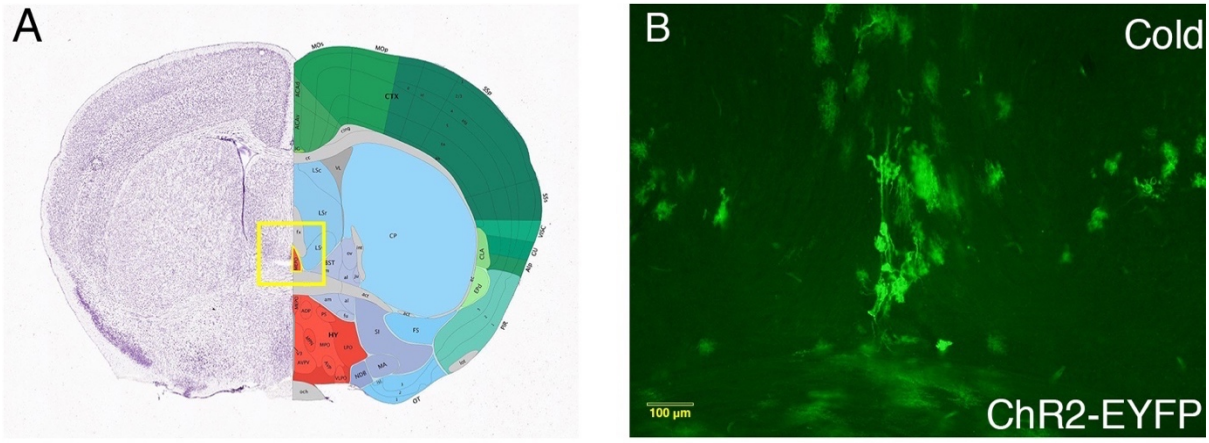

Figure 3.2.4 A. Image showing a coronal section at level 53 (Bregma 0.145) from an adult mouse brain with Nissl staining on the right hemisphere and atlas image on the left hemisphere. Areas of the hypothalamus are highlighted in red on the left hemisphere. The MnPO region is outlined in yellow, ventral and dorsal of the anterior commissure. The yellow box shows the area represented in the following 3 microscope images. Image taken from Allen Adult Mouse Brain Atlas (Lein et al., 2007). **B.** Representative image from 4°C group (n=4) of ChR2-EYFP labelling in green at 10x magnification (scale: 100 µm).

The temperature-sensitive neurons labelled in the MnPO using the double 4-OHT injection were much clearer, but the total number of neurons labelled using this method was only half of the total number labelled with endogenous c-Fos (Figures 3.1.1 and 3.1.2). While promising, this technique still requires optimisation before it can be reliably applied to temperature research.

3.3 Context-Temperature Association

The next aim of this project was to investigate the role of memory in temperature regulation. To understand if temperature information in encoded along with contextual memories, we developed a protocol to investigate whether physiological temperature responses could be artificially elicited via a context memory.

Mice were trained to associate a context with a temperature and then were tested in the absence of the temperature to see if the context alone could elicit metabolic responses seen in natural temperature exposure. First, mice were placed in Context A at room temperature (21°C) for 8 hours to record their baseline level metabolic responses. Following this, mice were given 3 days of cold exposure training in Context B. During

the cold exposure, the mice were placed in Context B at room temperature (21°C), after which the temperature ramped down to 4°C over the course of 2 hours, followed by an additional 6 hours at 4°C. The 2 hour ramp was a critical feature of the experimental protocol because it provided an "anticipatory" period during which the mice were aware of the context but the temperature had not yet reached 4°C. After the 3 days of cold exposure, mice were placed back in the cold-associated Context B, however the temperature remained at 21°C for the entirety of the exposure (Figure 3.3.1).

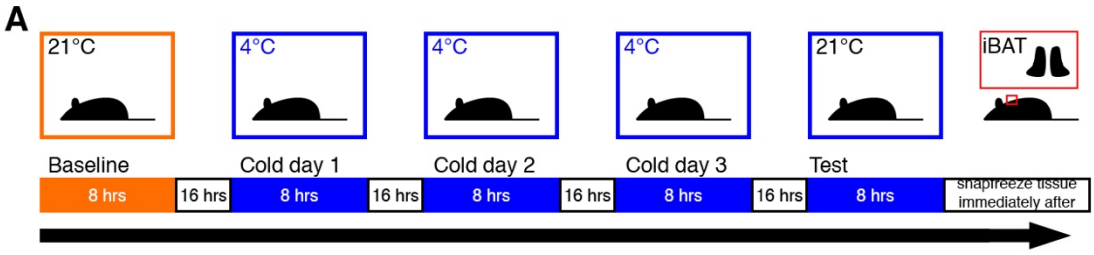

Figure 3.3.1: Anticipatory cold-context association protocol: schematic showing experimental timeline. Mice were first placed in Context A at 21°C for 8 hours (Baseline). This was followed by 3 days of cold training (4°C) in Context B for 8 hours (Cold days 1-3). Finally, mice were placed back in Context B but the temperature stayed at 21°C for 8 hours (Test day). Between each day of context and temperature exposure, mice were kept in their home cage for 16 hours. Immediately after mice were taken out of Context B on Test day, they were sacrificed and their intrascapular BAT (iBAT) was dissected and snapfrozen.

The hypothesis was that after 3 days of 4°C-context association training, mice would associate the Context B with a cold temperature. It was hypothesised that if the association was successful, mice would begin showing cold-defensive responses on the Test day in the 2 hour anticipatory ramp period at the beginning of the exposure. To determine this, the 2 hour temperature ramp periods were compared across Baseline, Cold and Test days (Figure 3.3.2).

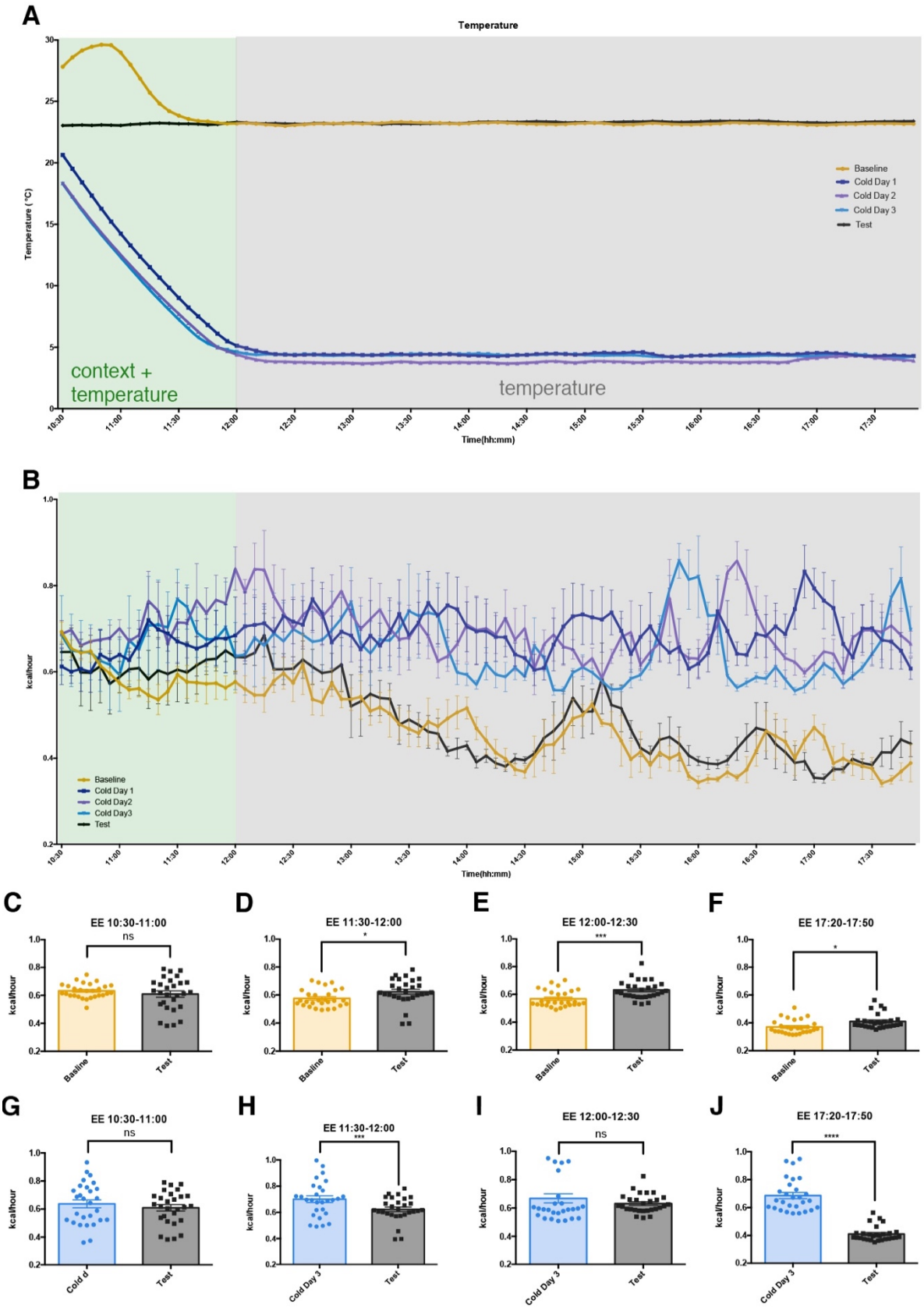

Figure 3.3.2 A. Time plot showing temperature measurements throughout 7 hours of recording. The first hour was removed due to calibration fluctuations. Baseline and Test days remain at a constant temperature of 21°C throughout the exposure. There was an unintended increase in the temperature of the Baseline exposure from 10:30-11:30. Cold days 1-3 begin at 21°C and the temperature decreases to 4°C

throughout the first 2 hours of the exposure. For the Cold days, the temperature ramp during the first 2 hours represents an "anticipatory period" during which the animals are exploring the context but the temperature has not yet reached the stable exposure condition (represented with green shading). Grey shading represents the time during which the temperature was stable. **B.** Time plot showing the EE response from the mice (n=4) across the different days (exposure conditions). Days are colour-coded and match the temperature depicted in A. Two-way ANOVA showed a significant effect of time (throughout exposure) ($p<0.0001$), a significant effect between different exposure conditions (days of protocol) ($p<0.0001$) and an interaction between time and day of exposure ($p<0.001$). **C.** Comparison of the EE values from 10:30-11:00, representing the beginning of the exposure, on the Baseline day and Test day. Paired t-test showed no significant difference between the days ($p=0.3704$). **D.** Comparison of the EE values from 11:30-12:00, representing the last 30 minutes of the anticipatory period, on the Baseline day and Test day. Paired t-test showed a significant difference between the days ($p=0.0167$). **E.** Comparison of the EE values from 12:00-12:30, representing the 30 minutes immediately after the anticipatory period, on the Baseline day and Test day. Paired t-test showed a significant difference between the groups ($p=0.0006$). **F.** Comparison of the EE values from 17:20-17:50, representing the end of the exposure, on the Baseline day and Test day. Paired t-test showed a significant difference between the groups ($p=0.0141$). **G.** Comparison of the EE values from 10:30-11:00, representing the beginning of the exposure, on the Cold day 3 and Test day. Paired t-test showed no significant difference between the days ($p=0.1007$). **H.** Comparison of the EE values from 11:30-12:00, representing the last 30 minutes of the anticipatory period, on the Cold day 3 and Test day. Paired t-test showed a significant difference between the days ($p=0.0005$). **I.** Comparison of the EE values from 12:00-12:30, representing the 30 minutes immediately after the anticipatory period, on the Cold day 3 and Test day. Paired t-test showed no significant difference between the groups ($p=0.2166$). **J.** Comparison of the EE values from 17:20-17:50, representing the end of the exposure, on the Cold day 3 and Test day. Paired t-test showed a significant difference between the groups ($p<0.0001$). Significance denoted in C-J as: ns $p>0.05$, * $p\leq 0.05$, ** $p\leq 0.01$, *** $p\leq 0.001$, **** $p\leq 0.0001$. Error bars show mean ± S.E.M.

Overall, the mice showed similar rates of EE on each day of the protocol at the beginning of the exposure. Then, after the 2 hour temperature ramp (context+temperature period) the EE values diverge into two groups based on the ambient temperature. In the latter portion of the exposure, the mice show similar EE values on the Baseline and Test day and these are divergent from the EE values recorded on the 3 Cold exposure days. A Repeated Measures Two-way ANOVA revealed a significant effect of the exposure condition (day of the protocol) on the EE rate throughout exposure ($p<0.0001$ for each day). There was a significant difference in the EE curves for Baseline compared with Cold day 3 ($p<0.0001$), reflecting that EE rates are different for room temperature and cold exposure conditions. There was no significant difference when comparing the curves for Baseline and Test ($p=0.4824$) or for Test and Cold day 3 ($p=0.5394$. Additionally, the rate of EE change over time of exposure (interaction effect) was significantly different when comparing Baseline and Cold day 3 ($p< 0.0001$) and when comparing Test and Cold day 3 ($p=0.0015$). But there was no interaction effect observed when comparing the EE rate on Baseline and Test days (0.8056).

In order to better understand the effect of the anticipatory period on the rate of EE, we specifically compared the EE values from the Test day with the EE values from the Baseline day and Cold day 3 to see which were more similar at specific time points (Figure 3.3.2 C-J). The first time point (10:30-11:00) represents when the mice were in the context but would not necessarily be showing a metabolic response to the context or the temperature. The second time point (11:30-12:00) was chosen as the last 30 minutes of the anticipatory period to test whether the EE rate had changed at this point due to the context. The third time point (12:00-12:30) represents the time immediately after the anticipatory period when the temperature is stable but the EE rate might still be reflecting the response to the context. Finally, the last time point (17:20-17:50) reflects the EE rate in response to the temperature alone.

At the beginning of the exposure there is no significant difference between the Test and Baseline or Test and Cold day 3 rates of EE. However, the values diverge throughout the 2-hour anticipatory period and the Test day EE values hover between the Baseline and Cold day values. Immediately after the anticipatory period, the Test day EE rates are significantly higher than those of the Baseline day rates, which suggests that the mice are activating cold-defensive metabolic responses at this time. This is corroborated by the finding that there is no significant difference between the Cold day 3 and Test day EE rates during this same time point. The context is the only difference between the Baseline and Test days, and therefore the increased EE rates seen in the Test day signify that the mice associated Context B with a cold temperature and were eliciting an increased metabolic rate in anticipation of a cold exposure.

Once the temperature has stabilised after the anticipatory period, the Baseline and Test day EE rates follow the same trajectory for the rest of the exposure. This signifies a shift when the metabolic responses to the ambient temperature override the anticipatory metabolic responses evoked by the context.

Taken together, these results suggests that mice can associate a context with an aversive temperature, and this association can lead to an activation of cold-defensive responses, such as increased EE. This metabolic change is seen in response to context exposure and in the absence of ambient temperature change, which signifies that the metabolic change is employed as an anticipatory cold response to the cold-associated context.

3.4 Extended effect of cold

The increased EE seen on the Test day (Figure 3.3.2) could have been due to an extended effect of 3 days of cold exposure on the metabolic response. Therefore, to rule this out as a possible confounding variable, a second Baseline day was added to the protocol after the 3 cold exposure days and before the Test day to give the mice an additional 24 hours to recover from any extended cold effects (Figure 3.4.1). The Baseline 2 day also provided a context specificity control to ascertain whether there were any effects of generalisation across Context A and B that would lead to an increased EE seen on the Test day.

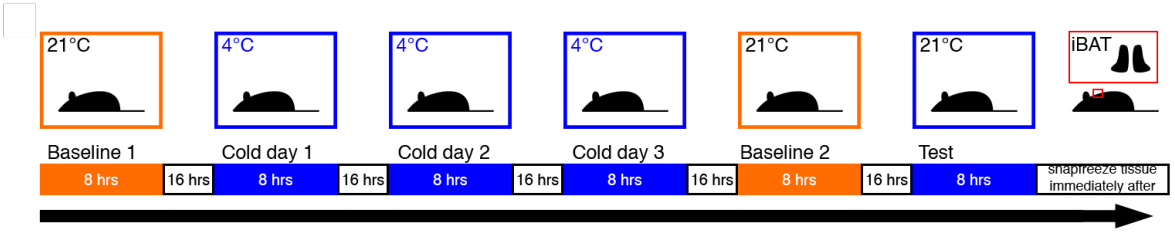

Figure 3.4.1: Anticipatory cold-context association protocol: schematic showing experimental timeline, which is similar to figure 3.3.1 except with an additional Baseline 2 day added after Cold day 3 and before Test day.

To investigate the potential extended effect of cold exposure, the EE values for the Test day of the groups with and without Baseline 2 were compared. The group without Baseline 2 (Figure 3.3.1) had 16 hours after Cold exposure and before Test day, whereas the group with a Baseline 2 (Figure 3.4.1) had 40 hours after Cold exposure and before Test day (Figure 3.4.2).

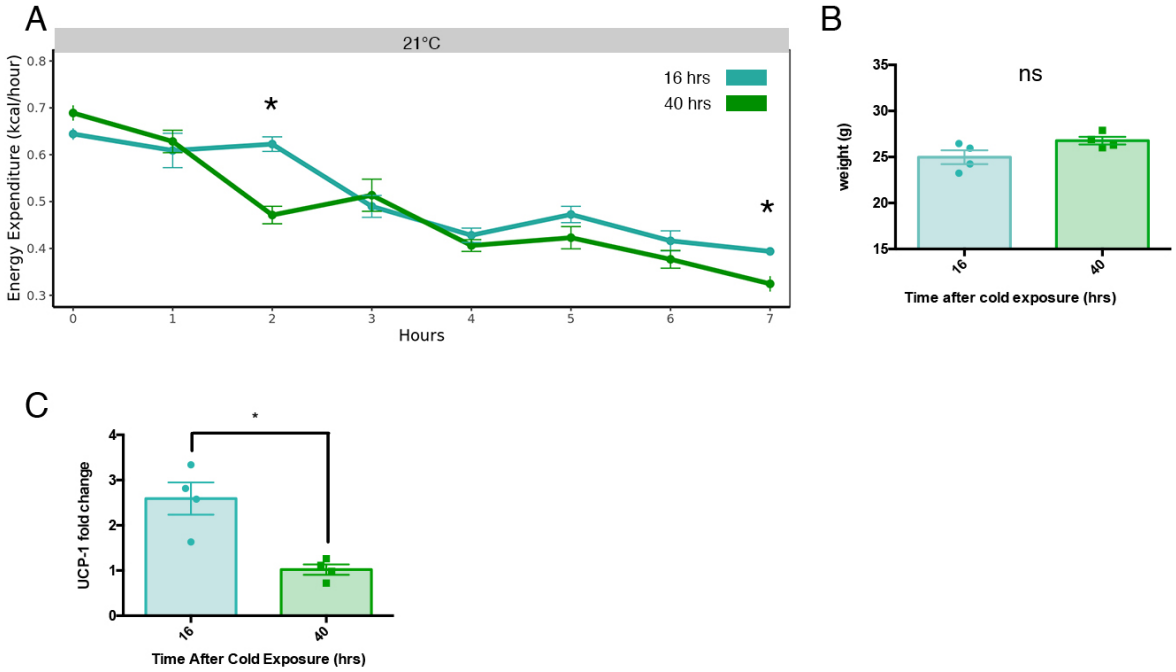

Figure 3.4.2:A. Time plot for EE on Test day when the Test day was 16 hours (n=4) or 40 hours (n=4) after 3 days of cold exposure. The grey bar at the top shows that the temperature was 21°C for the entire exposure. EE of the 16 hour group is significantly higher than the 40 hour group at hours 2 and 7 of the exposure (p=0.0090 and p=0.0097, respectively). **B.** Weights of both groups were measured before the exposure on Test day. A two-tailed unpaired t-test showed that there was no significant difference between the weights of the groups (p=0.0936). **C.** UCP-1 upregulation compared for 16 hour and 40 hour group. A two-tailed unpaired t-test showed that the 16 hour group had significant upregulation of UCP-1 compared to the 40 hours group (p=0.0171). Error bars show mean ± S.E.M.

In the group that was tested 16 hours after cold exposure, the EE was higher at hours 2 and 7, which represents a metabolic effect of the extended cold exposure. This effect was more pronounced in the analysis of BAT thermogenesis, quantified based on the upregulation of UCP-1 mRNA. The group tested 16 hours after 3 days of cold exposure showed increased UCP-1 mRNA expression compared to the group tested 40 hours after 3 days of cold exposure. This signifies that 16 hours after the 3 days of cold exposure, mice may have still been in a thermogenic state.

3.5 Role of contextual association in thermoregulatory response

Since the BAT thermogenesis levels were lower after 40 hours compared to 16 hours, we analysed whether the anticipatory response of EE seen in the 16 hour group would still be present on the Test day in the 40 hour group. The anticipatory response shown by an increased EE in the first 2 hours of exposure was still present even in the 40 hour

group, where the extended effect of cold did not seem to have as large of an effect (Figure 3.5.1).

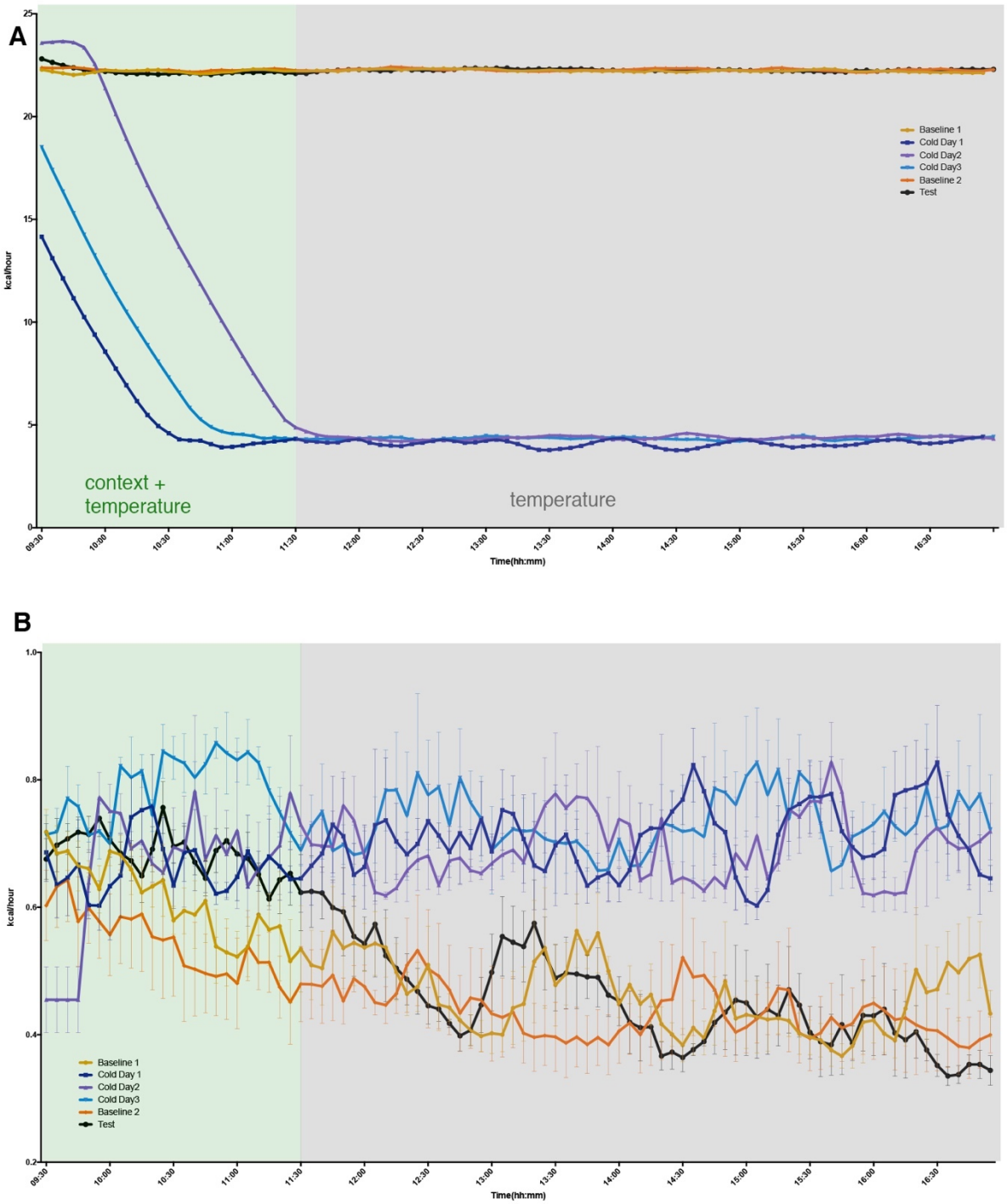

Figure 3.5.1:A. Time plot showing temperature measurements throughout 7 hours of recording. The first hour was removed due to calibration fluctuations. Baseline 1, Baseline 2, and Test days remain at a constant temperature of 21°C throughout the exposure. Cold days 1-3 begin at 21°C and the temperature decreases to 4°C throughout the first 2 hours of the exposure. The temperature ramp was unintentionally shifted between the different cold days. For the Cold days, the temperature ramp during the first 2 hours represents an "anticipatory period" during which the mice are exploring the context but the temperature has not yet reached the stable exposure condition (represented with green shading). Grey shading

represents the time during which the temperature was stable. **B.** Time plot showing the EE response from the mice (n=4) across the different days (exposure conditions). Days are colour-coded and match the temperature depicted in A. Repeated measures Two-way ANOVA showed a significant effect of time (throughout exposure) ($p<0.0001$), a significant effect between different exposure conditions (days of protocol) ($p<0.0001$) and an interaction between time and exposure condition ($p<0.001$). Error bars show mean ± S.E.M.

The results from the protocol with Baseline 2 are similar to those from the protocol without the Baseline 2 day. The EE rates from each day of the protocol are similar at the beginning of the exposure and then diverge into two groups throughout the exposure based on the ambient temperature. A Repeated Measures Two-way ANOVA revealed a significant effect of the exposure condition (day of the protocol) on the EE rate throughout exposure ($p<0.0001$ for Baseline 1, Cold day 1, Cold day 2, Cold day 3, and Baseline 2; $p=0.0010$ for Test). When comparing between the days, the curves were significantly different for Baseline 2 compared to Cold day 3 ($p=0.0037$) and Test day compared to Cold day 3 ($p=0.0002$). However, there was no significant difference between the rates of EE on the Baseline 2 and Test days ($p=0.4115$). The rate of EE change over time of exposure (interaction effect) was significantly different when comparing Baseline 2 and Test day EE rates ($p< 0.0001$) and when comparing Test and Cold day 3 ($p< 0.0001$) EE rates. But there was no interaction effect observed when comparing the EE rate for Baseline 2 and Cold day 3 ($p=0.1292$).

To look more closely at the anticipatory effect on the rate of EE, Test day EE values were compared with the values from Baseline 1, Baseline 2, and Cold day 3 at specific time points throughout the exposure (Figure 3.5.2). The aim was to understand whether the Test day EE values were more similar to the Baseline day EE or to the Cold day 3 EE. The Test and Baseline day EE rates are not significantly different at the first time point, but in the last 30 minutes of the anticipatory period and for the 30 minutes immediately after the anticipatory period, the Test day EE values are significantly higher than the Baseline day values. This signifies that the mice are showing cold-defensive behaviours, which are reflected as a higher rate of EE. At the end of the exposure, the Test day EE rates are significantly lower than those of the Baseline day. This result signifies that after the anticipatory period on the Test day, the EE rate decreased, reflecting that the mice were now responding to the ambient temperature instead of the context association.

Comparisons between the Baseline 2 and Test day EE rates across the four time points reveal the same results as the comparisons between Baseline 1 and Test day EE rates. However, when comparing the Cold day 3 and Test day EE, the results are the opposite of what was found in the Baseline day 1 and Baseline day 2 EE comparisons with the Test day. There was no significant difference between the Cold day 3 and Test day EE values in the first time point, but for the following three time points the Test day rate of EE was significantly lower than the rate of EE on Cold day 3. This signifies that the rate of EE on the Test day was higher than the Baseline days but lower than the Cold days. These results suggest that the mice successfully associated the Context B with a cold temperature and therefore showed cold-defensive metabolic responses when placed in this context on the Test day (reflected by higher Test day EE values than Baseline day values). However, the metabolic response elicited by the context alone was not as strong as the metabolic response to the natural cold temperature exposure (reflected by lower EE values on Test day than on Cold day 3).

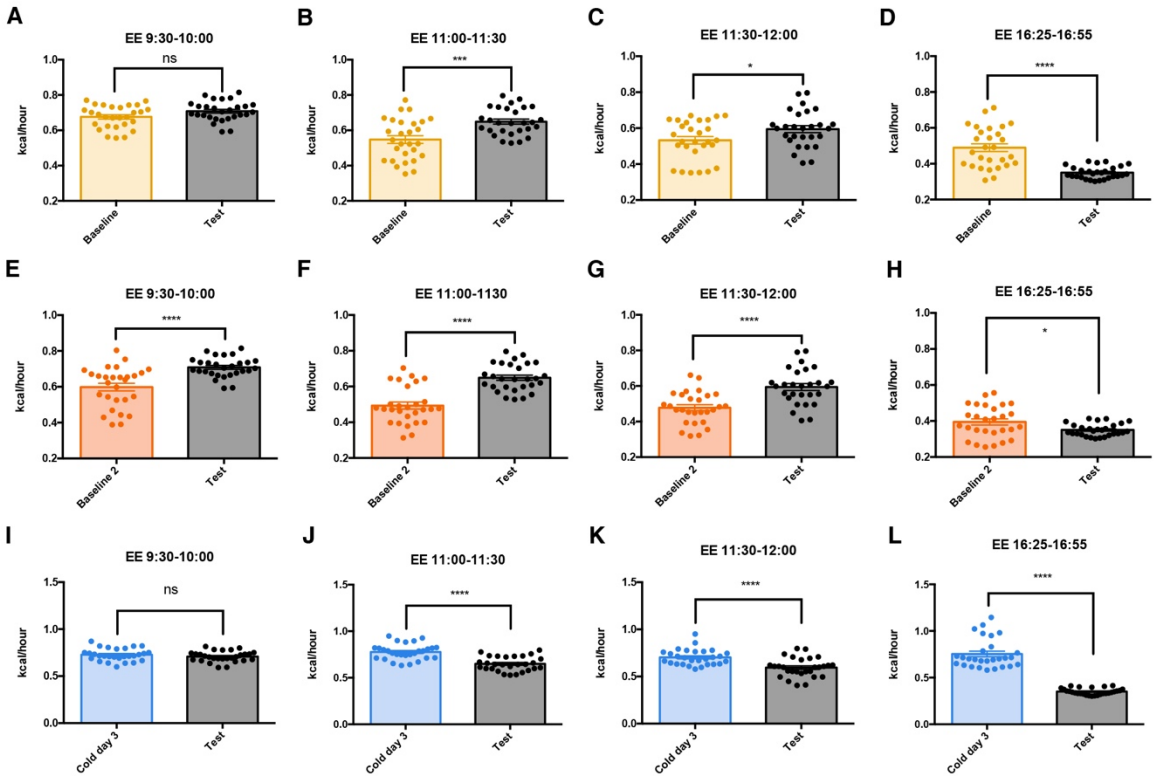

Figure 3.5.2: A. Comparison of the EE values from 9:30-10:00, representing the beginning of the exposure, on the Baseline day and Test day. Paired t-test showed no significant difference between the days (p=0.0937), (n=4). **B.** Comparison of the EE values from 11:00-11:30, representing the last 30 minutes of the anticipatory period, on the Baseline day and Test day. Paired t-test showed a significant difference between the days (p=0.0002), (n=4). **C.** Comparison of the EE values from 11:30-12:00,

representing the 30 minutes immediately after the anticipatory period, on the Baseline day and Test day. Paired t-test showed a significant difference between the groups ($p=0.0258$), ($n=4$). **D.** Comparison of the EE values from 16:25-16:55, representing the end of the exposure, on the Baseline day and Test day. Paired t-test showed a significant difference between the groups ($p<0.0001$), ($n=4$). **E.** Comparison of the EE values from 9:30-10:00, representing the beginning of the exposure, on the Baseline 2 and Test day. Paired t-test showed a significant difference between the days ($p<0.0001$), ($n=4$). **F.** Comparison of the EE values from 11:00-11:30, representing the last 30 minutes of the anticipatory period, on the Baseline 2 and Test day. Paired t-test showed a significant difference between the days ($p<0.0001$), ($n=4$). **G.** Comparison of the EE values from 11:30-12:00, representing the 30 minutes immediately after the anticipatory period, on the Baseline 2 and Test day. Paired t-test showed a significant difference between the groups ($p<0.0001$), ($n=4$). **H.** Comparison of the EE values from 16:25-16:55, representing the end of the exposure, on the Baseline 2 and Test day. Paired t-test showed a significant difference between the groups ($p=0.0357$), ($n=4$). **I.** Comparison of the EE values from 9:30-10:00, representing the beginning of the exposure, on the Cold day 3 and Test day. Paired t-test showed no significant difference between the days ($p=0.2670$), ($n=4$). **J.** Comparison of the EE values from 11:00-11:30, representing the last 30 minutes of the anticipatory period, on the Cold day 3 and Test day. Paired t-test showed a significant difference between the days ($p<0.0001$) ($n=4$). **K.** Comparison of the EE values from 11:30-12:00, representing the 30 minutes immediately after the anticipatory period, on the Cold day 3 and Test day. Paired t-test showed a significant difference between the groups ($p<0.0001$), ($n=4$). **L.** Comparison of the EE values from 16:25-16:55, representing the end of the exposure, on the Baseline 2 and Test day. Paired t-test showed a significant difference between the groups ($p<0.0001$), ($n=4$). Significance denoted in A-L as: ns $p>0.05$, * $p\leq 0.05$, ** $p\leq 0.01$, *** $p\leq 0.001$, **** $p\leq 0.0001$. Error bars show mean ± S.E.M.

To see whether the results were reproducible across different metabolic measures, the carbon dioxide emission was compared across each day of the protocol (Figure 3.5.3).

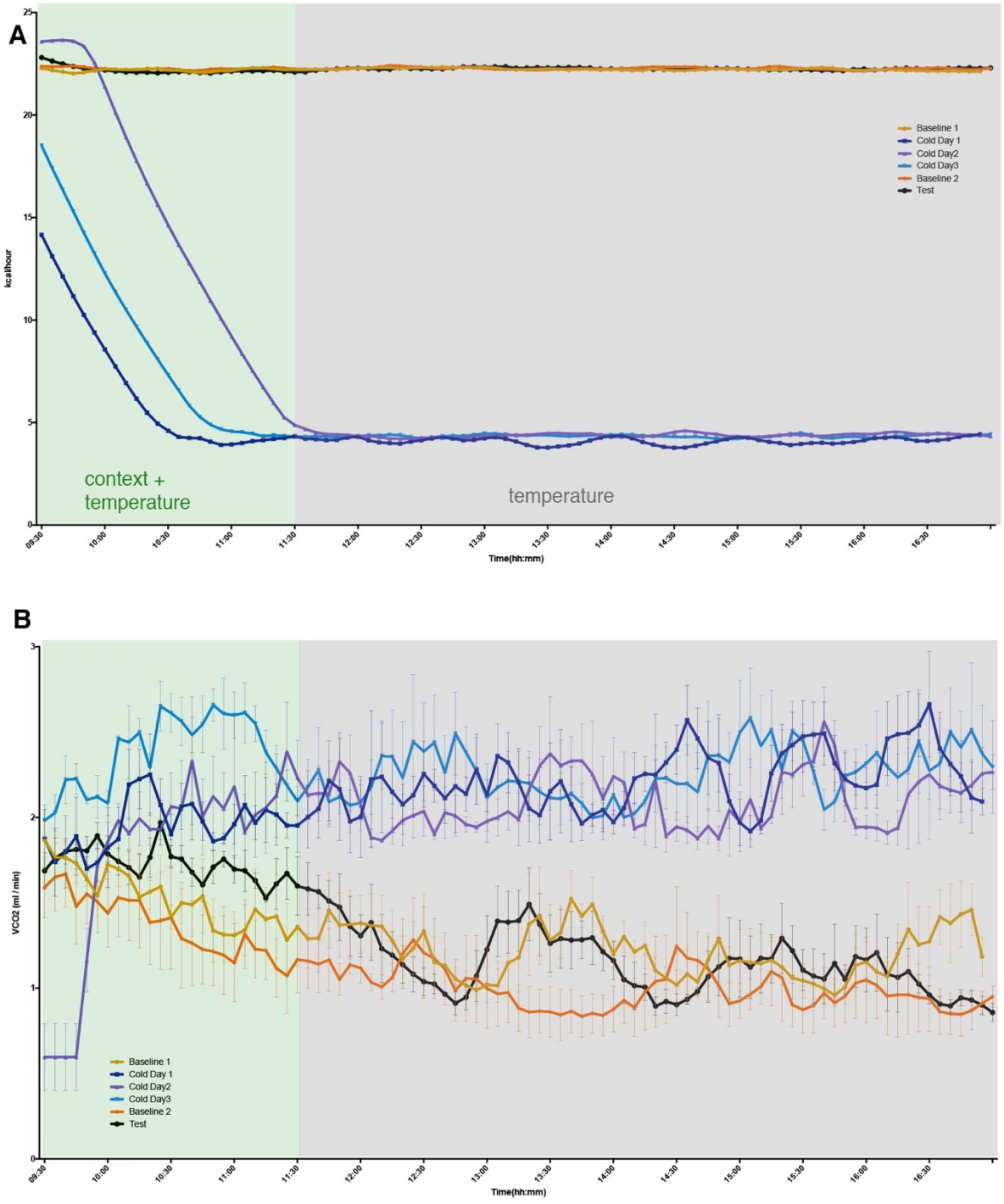

Figure 3.5.3: A. Time plot showing temperature measurements throughout 7 hours of recording. The first hour was removed due to calibration fluctuations. Baseline 1, Baseline 2, and Test days remain at a constant temperature of 21°C throughout the exposure. Cold days 1-3 begin at 21°C and the temperature decreases to 4°C throughout the first 2 hours of the exposure. The temperature ramp was unintentionally shifted between the different cold days. For the Cold days, the temperature ramp during the first 2 hours represents an "anticipatory period" during which the animals are exploring the context but the temperature has not yet reached the stable exposure condition (represented with green shading). Grey shading represents the time during which the temperature was stable. **B.** Time plot showing the CO_2 emission from the mice (n=4) across the different days. Days are colour-coded and match the temperature depicted in A. Two-way ANOVA showed a significant effect of time (throughout exposure) (p=0.0001),

a significant effect between different exposure conditions (days of protocol) ($p<0.0001$) and an interaction between time and exposure condition ($p<0.001$).

The overall trends seen in carbon dioxide emission rate on each day of the protocol were similar to the trends of EE. A Repeated Measures Two-way ANOVA revealed a significant effect of the exposure condition (day of the protocol) on the EE rate throughout exposure ($p<0.0001$ for Baseline 1, Cold day 1, Cold day 2, Cold day 3, and Baseline 2; $p=0.0076$ for Test). When comparing between the days, the curves were significantly different for Baseline 2 compared to Cold day 3 ($p=0.0006$) and Test day compared to Cold day 3 ($p<0.0001$). However, there was no significant difference between the rates of EE on the Baseline 2 and Test days ($p=0.2425$). The rate of EE change over time of exposure (interaction effect) was significantly different when comparing Baseline 2 and Test day EE rates ($p=0.0008$), when comparing Test and Cold day 3 ($p< 0.0001$) EE rates, and when comparing Baseline 2 and Cold day 3 ($p=0.0002$).

To investigate the effect of the anticipatory period, we compared the Test day CO_2 emission rates to Baseline 1, Baseline 2, and Cold day 3 CO_2 emission rates. As in the EE data, the Test day CO_2 emission values are significantly higher than those of the Baseline 1 and Baseline 2 day values at most time points throughout the exposures. However, the CO_2 emission rate do not reflect as strong of an anticipatory effect as was shown in the EE data. This is shown by the lack of difference between the Baseline 1 and Test day CO_2 rate immediately after the anticipatory period. Taken together, the higher CO_2 emission rates seen on the Test day when compared to the Baseline days reflects that there was a context-elicited cold-defensive response occurring on the Test day.

Comparison of the Cold day 3 and Test day CO_2 emission rates revealed a similar effect as seen in the EE data. The Test day CO_2 emission rates are significantly lower than the Cold day 3 CO_2 emission rates throughout the entire exposure. This signifies that the context-elicited metabolic response was not as strong as the natural metabolic response to cold temperature exposure.

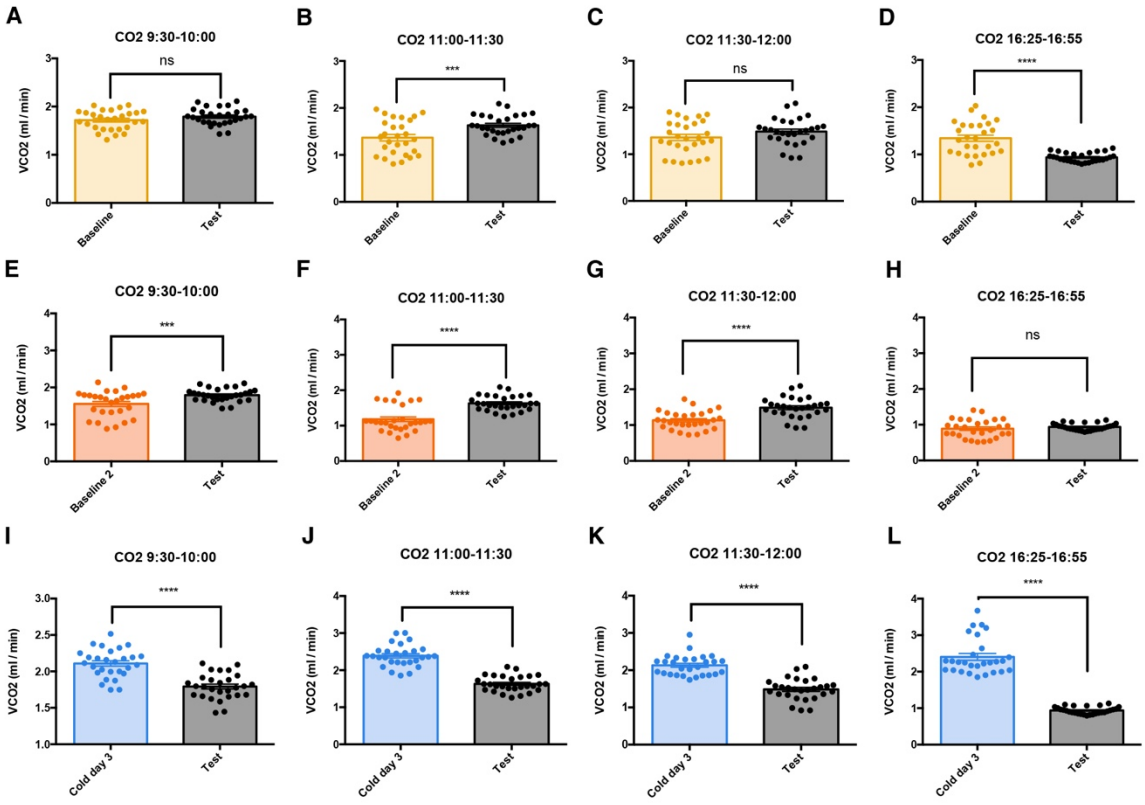

Figure 3.5.4: A. Comparison of the CO_2 values from 9:30-10:00, representing the beginning of the exposure, on the Baseline day and Test day. Paired t-test showed no significant difference between the days (p=0.1921), (n=4). **B.** Comparison of the CO_2 values from 11:00-11:30, representing the last 30 minutes of the anticipatory period, on the Baseline day and Test day. Paired t-test showed a significant difference between the groups (p=0.0008), (n=4). **C.** Comparison of the CO_2 values from 11:30-12:00, representing the 30 minutes immediately after the anticipatory period, on the Baseline day and Test day. Paired t-test showed no significant difference between the groups (p=0.0960), (n=4). **D.** Comparison of the CO_2 values from 16:25-16:55, representing the end of the exposure, on the Baseline day and Test day. Paired t-test showed a significant difference between the groups (p<0.0001), (n=4). **E.** Comparison of the CO_2 values from 9:30-10:00, representing the beginning of the exposure, on the Baseline 2 and Test day. Paired t-test showed a significant difference between the days (p=0.0007), (n=4). **F.** Comparison of the CO_2 values from 11:00-11:30, representing the last 30 minutes of the anticipatory period, on the Baseline 2 and Test day. Paired t-test showed a significant difference between the days (p<0.0001), (n=4). **G.** Comparison of the CO_2 values from 11:30-12:00, representing the 30 minutes immediately after the anticipatory period, on the Baseline 2 and Test day. Paired t-test showed a significant difference between the groups (p<0.0001), (n=4). **H.** Comparison of the CO_2 values from 16:25-16:55, representing the end of the exposure, on the Baseline 2 and Test day. Paired t-test showed no significant difference between the groups (p=0.4105), (n=4). **I.** Comparison of the CO_2 values from 9:30-10:00, representing the beginning of the exposure, on the Cold day 3 and Test day. Paired t-test showed a significant difference between the days (p<0.0001), (n=4). **J.** Comparison of the CO_2 values from 11:00-11:30, representing the last 30 minutes of the anticipatory period, on the Cold day 3 and Test day. Paired t-test showed a significant difference between the days (p<0.0001), (n=4). **K.** Comparison of the CO_2 values from 11:30-12:00, representing the 30 minutes immediately after the anticipatory period, on the Cold day 3 and Test day. Paired t-test showed a significant difference between the groups (p<0.0001), (n=4). **L.** Comparison of the CO_2 values from 16:25-16:55, representing the end of the exposure, on the Baseline 2 and Test day. Paired t-test showed a significant difference between the groups (p<0.0001), (n=4). Significance denoted in A-L as: ns p>0.05, * p≤ 0.05, ** p≤ 0.01, *** p≤ 0.001, **** p≤ 0.0001. Error bars show mean ± S.E.M. Error bars show mean ± S.E.M.

3.6 Effect of sex on metabolic rate in different temperature conditions

The next aim of this project was to investigate how thermoregulation is affected by different variables, including sex of animal and time of day. Specifically, we focused on how these different states affect EE in both room temperature and cold exposure.

The first question addressed was whether sex has an effect on EE. The same male mice that went through the anticipatory cold-context association protocol shown in Figure 3.4.1 were compared with a group of female mice that underwent the same experimental design. The rate of EE from both groups was compared on Baseline day 1 (21°C) and Cold day 1 (4°C).

The group of males showed significantly higher EE at hour 1. However, since the females weigh less we would expect them to expend less energy (Figure 3.6.1). Therefore, we cannot say that the significance is due to sex.

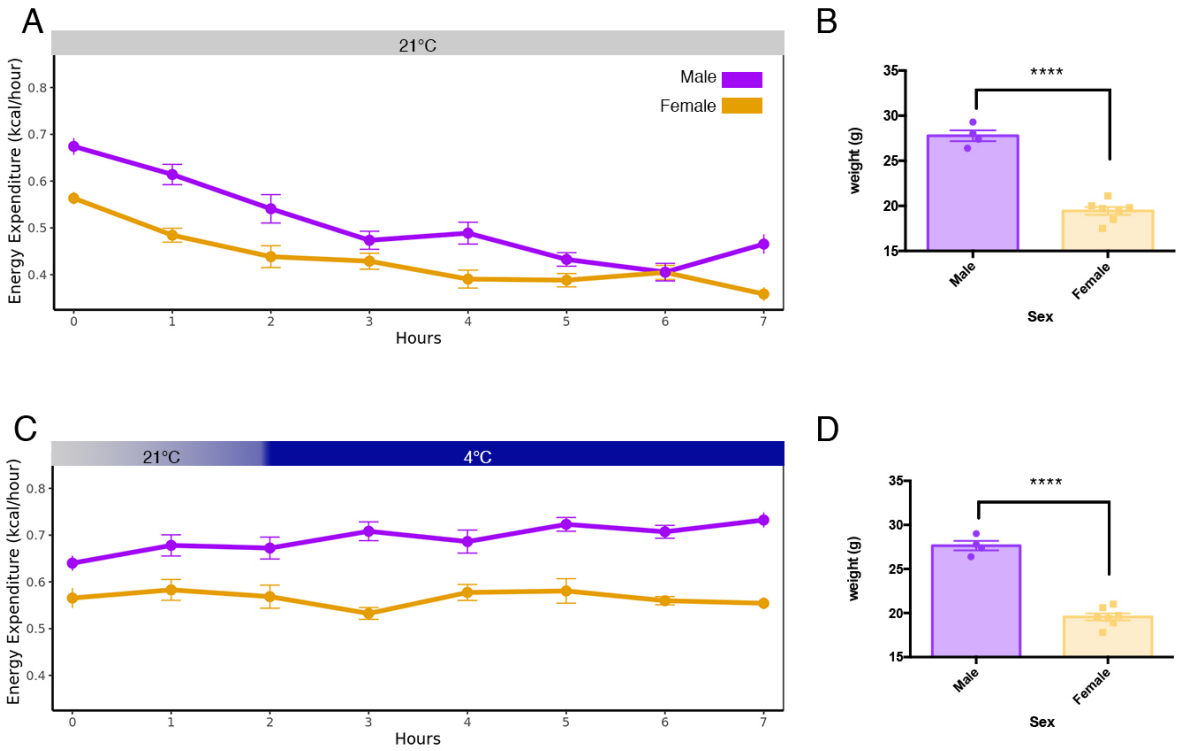

Figure 3.6.1: A. Time plot from CalR for male(n=4) and female (n=7) EE at room temperature (21°C). Bar at top shows temperature throughout reading (21°C for entire exposure). Purple line in graph represents males and yellow represents females. EE is higher for males throughout, with a significant difference at hour 1 (p=0.0364). Error bars show mean ± S.E.M. **B.** Weights of females and males taken before Baseline day (21°C). A two-tailed unpaired t-test showed males weighed significantly more than females (p<0.0001). Error bars show mean ± S.E.M. **C.** Time plot from CalR for male and female EE on

Cold day 1 (4°C). Bar at top shows temperature throughout recording (starts at 21°C and then ramps down to 4°C degrees by hour 2). EE is higher for males throughout, with a significant difference at hour 2 ($p=0.0445$), hour 3 ($p=0.0012$), hour 4 ($p=0.0073$), hour 5 ($p=0.0298$), hour 6 ($p<0.001$), hour 7 ($p=0.0011$). Error bars show mean ± S.E.M. **D.** Weights of females and males taken before Cold day 1 (4°C) exposure. A two-tailed unpaired t-test shows that males weighted significantly more than females ($p<0.0001$). Bar at top shows temperature throughout reading (starts at 21°C and then ramps down to 4°C by hour 2). Error bars show mean ± S.E.M.

To measure the level of BAT thermogenesis occurring in each group, mice were sacrificed 40 hours after 3 days of cold exposure, and the intrascapular brown adipose tissue (iBAT) was harvested. UCP-1 mRNA was measured in the iBAT post-mortem using RT qPCR analysis.

There was no significant difference between the levels of UCP-1 mRNA in males and females (Figure 3.6.2). This supports previous findings showing that at cold temperature the UCP-1 levels were the same for males and females (Quevedo et al., 1998).

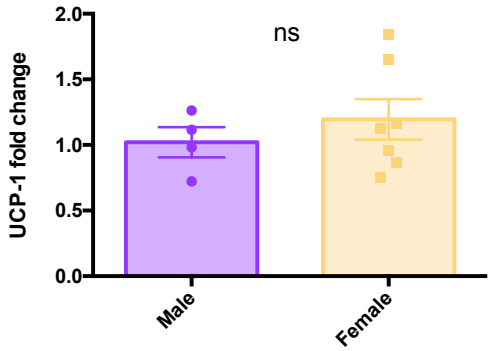

Figure 3.6.2: UCP-1 upregulation compared for females (n=7) and males (n=4). A two-tailed unpaired t-test revealed that there was no significant difference between the groups ($p=0.3874$). Error bars show mean ± S.E.M.

3.7 Influence of time of day on metabolic rate in different temperature conditions

The next experimental goal was to investigate the effect of time of day on EE. The same male mice that underwent the anticipatory cold-context association protocol in Figure 3.4.1 were compared to a group of male mice that underwent the same protocol, except during night time instead of daytime hours. The rates of EE for these two groups were compared on the Baseline day 1 (21°C) and the Cold day 1 (4°C) to understand whether mice respond to cold exposure differently depending on the time of day.

Overall, there were not large differences in the rate of EE for the night time and daytime groups. However, the timing of when EE increases and when it decreases is opposite for the groups, which is what we would expect based on circadian rhythms. On Baseline day 1 (21°C), the night time group shows higher EE throughout the second half of the exposure, however this is not to a significant level. On the Cold day 1 (4°C), the overall rhythm of EE is opposite for the daytime and night time groups. The night time group begins at significantly higher EE than the daytime group and throughout the exposure the EE rate decrease. Contrastingly, the EE rates for the daytime group begin lower and increase in the second half of the exposure (Figure 3.7.1).

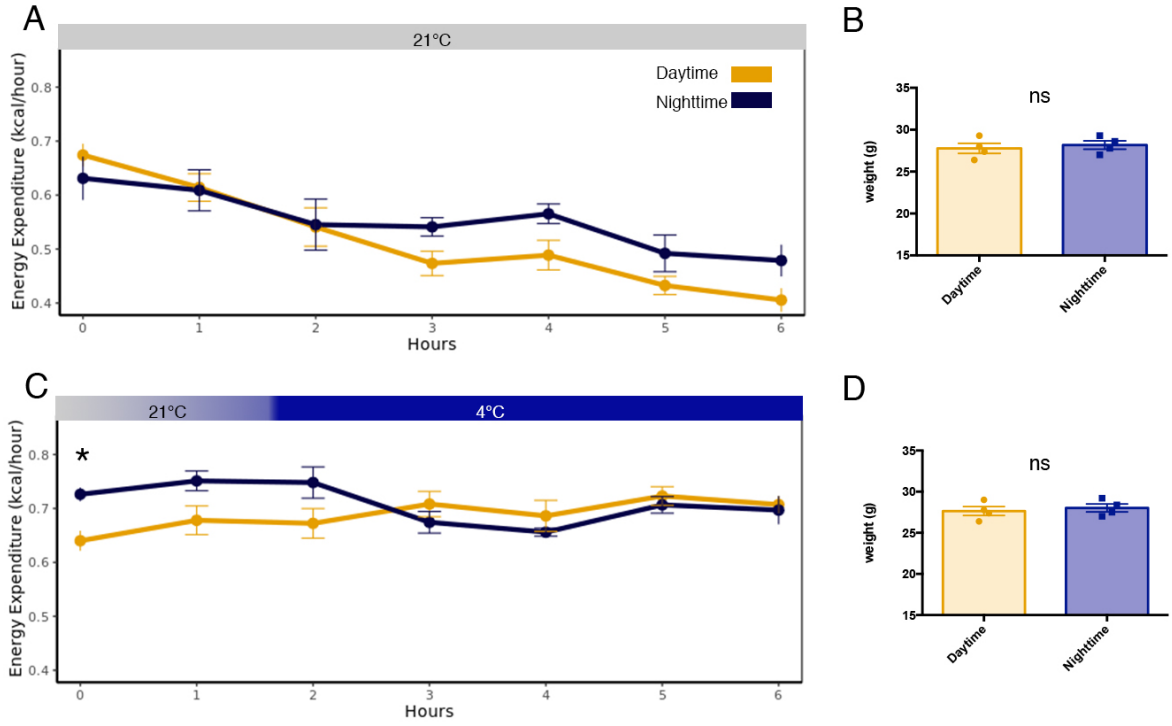

Figure 3.7.1: A. Time plot for daytime (n=4) and night time (n=4) EE at room temperature (21°C). Bar at top shows temperature throughout recording (21°C for entire exposure). Yellow line in graph represents daytime and blue represents night time. At hour 1 and hour 3 there are significant differences (p=0.0052 and p=0.0153, respectively), however there is also an interaction effect of the mass effect and group effect at these time points, so therefore the significance result is inconclusive. Error bars show mean ± S.E.M. **B.** Weights of both groups before Baseline day (21°C). A two-tailed unpaired t-test revealed that there was no significant difference (p=0.6288). Error bars show mean ± S.E.M. **C.** Time plot for daytime (n=4) and night-time (n=4) EE on Cold day 1 (4°C). Bar at top shows temperature throughout recording (starts at 21°C and then ramps down to 4°C degrees by hour 2). EE is higher for night time group in the first half of the exposure but switches to lower in the second half of the exposure. At hour 0 the night time group has significantly higher EE than the daytime group (p=0.0480). At hour 4 there is a significant difference between the groups (p=0.0288), however there is also an interaction effect of the mass effect and group effect at hour 4, so therefore the significance result is inconclusive. Error bars show mean ± S.E.M. **D.** Weights of both groups before Cold day 1 (4°C). A two-tailed unpaired t-test shows there was no significant difference (p=0.6239). Error bars show mean ± S.E.M.

To investigate whether there was an effect of time of day on the level of BAT thermogenesis occurring in each group, mice were sacrificed 40 hours after 3 days of cold exposure, and the intrascapular brown adipose tissue (iBAT) was harvested. UCP-1 mRNA was measured in the iBAT post-mortem using RT qPCR analysis (Figure 3.7.2). Analysis of UCP-1 mRNA showed no significant difference between the groups, signifying that the time of day doesn't affect the level of thermogenesis.

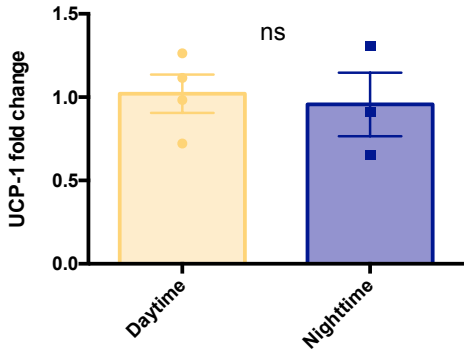

Figure 3.7.2: UCP-1 upregulation compared for males during night time (n=4) and day time(n=4). A two-tailed unpaired t-test showed no significant difference between the groups (p=0.7886). Error bars show mean ± S.E.M.

Chapter 4: Discussion

4.1 Application of engram technology

The advent of engram labelling technology paired with optogenetics provided the opportunity to label and manipulate specific neurons that are activated during a unique learning experience. The application of engram technology to temperature research would allow investigation of innate responses in the same way that we can currently interrogate learned experiences. The ability to label and manipulate temperature-sensitive neurons and circuitry would provide more clarity about the different components required for activation of innate responses. Using a similar method to study both innate and learned responses would also allow investigation into the shared mechanisms between these two types of information. Therefore, one aim of this project was to apply engram labelling technology to thermoregulation research, representing the first attempt to do this.

Engram labelling was first used in the hippocampus to label the specific cells associated with a memory. When adapting this technology to temperature research, there are many variables that need to be considered, including the viability of the technique in a new brain region with different types of cells. The brain region of interest in this project was the MnPO due to its significance in temperature regulation. Previous research has successfully utilised c-Fos as a marker of recent activity in the MnPO and therefore, this research applied the same method to label the specific hypothalamic region. This research verified that there are temperature sensitive neurons in the MnPO that can be labelled using c-Fos as a marker of recent activity. In future research, it would be beneficial to compare other methods of activity dependent labelling, such as Arc and zif268 IEG expression, with c-Fos to see which method proves the most effective in labelling cells in the MnPO.

After successfully labelling temperature sensitive neurons in the MnPO with c-Fos, it was hypothesised that these neurons could be tagged using the tTA engram labelling system. However, when this was attempted the post-mortem immunohistochemistry revealed a very small number of neurons labelled in the MnPO. There was some

labelling identified in the peripheral regions to the MnPO, but the pattern of labelling suggested that there was massive cell death within the MnPO.

Cell death has been reported as a result of the engram labelling technique, due to overexpression of c-Fos protein. In the original successful application of engram labelling technology, the experience used to label the memory lasted a relatively short time, less than 15 minutes. However, in our experiments, the temperature exposure lasted for 4 hours, which could have caused overexpression of c-Fos in the MnPO during this time. Therefore, we hypothesised that such a long exposure time for the labelling window could have led to cell death, which would result in a lack of labelling in the MnPO.

The next approach was to use a Cre-based method for labelling the temperature-sensitive neurons. The results from this engram labelling method were much more promising, with much clearer labelling in the MnPO. However, in comparison to the endogenous c-Fos activated in the MnPO region after temperature exposure, we were still seeing a small percent of temperature-sensitive neurons labelled in the MnPO using the Cre-based engram strategy.

As with the tTA labelling strategy, there are many factors that could influence the efficiency of this method. The system used in this research relies on the use of fosTRAPxAi32 transgenic mice combined with 4-OHT injection to label the neurons active in a specific time window. The first approach was to use only one injection of 4-OHT immediately after the temperature experience, but this resulted in very low levels of labelling. Adding a second 4-OHT injection 2 hours post-exposure provided promising results for labelling a higher percent of active neurons in the MnPO after temperature exposure. While the labelling levels were not high enough to be confident that we were labelling all active neurons, this approach is very promising for future research.

There is evidence that 4-OHT injection can be administered before or after stimulus exposure and therefore one potential for optimisation could be to test the timing of 4-OHT injection to see which is the most relevant for this application (Cazzulino et al., 2016). Similar to the tTA labelling strategy, the other area for optimisation could be the

timing of exposure. To ensure that temperature-reactive neurons are being labelled, the temperature exposure window could be reduced. Taken together, these results can inform and direct future investigation into the optimisation of engram technology for temperature research.

4.2 Developing a protocol for context-temperature association

Another objective of this research was to investigate the different factors influencing temperature regulation. Specifically, it was hypothesised that memory plays a role in thermoregulation. It would be advantageous for animals to remember a place where they experienced an aversive temperature condition and if ever exposed to the place again they could immediately activate thermoregulatory responses to defend their core temperature. Therefore, one aim of this project was to investigate whether a context could be associated with an aversive temperature, and whether the temperature-paired context alone could elicit a temperature response. To probe these questions, it was necessary to develop a protocol to test whether context memory could affect the metabolic responses associated with temperature regulation.

This research successfully developed a Pavlovian experimental paradigm for training mice to associate a temperature with a context. This protocol included a 2 hour anticipatory period at the beginning of each exposure, during which mice were placed in a context but not yet exposed to an aversive temperature. By measuring the EE and CO_2 emission during this time, it was possible to compare the effect of the context without the influence of the temperature. After 3 days of cold training in a specific context, mice were tested in the context alone without the cold temperature. Mice showed a trend towards higher EE during and immediately after the anticipatory period, which signifies an increased metabolic rate was activated in reaction to the context alone. This result indicates that mice are able to associate a context with a temperature, and that the context alone is sufficient to induce metabolic effects seen in the natural temperature condition. Furthermore, this result suggests that memory plays a role in temperature regulation.

4.3 Factors influencing thermoregulation

Using the anticipatory cold-context association protocol, we investigated other factors influencing thermoregulation. To understand whether sex has an effect on the rate of EE at both room temperature and cold conditions, we examined the level of thermogenesis in males and females using the anticipatory cold-context association protocol. Our results show that there were no significant differences in the level of UCP-1 mRNA upregulation and the rate of EE for males and females at both cold and room temperature conditions. This finding suggests that there is not a large effect of sex on the thermogenic response. However, previous research done by Quevedo et al found that females induce higher levels of thermogenesis at room temperature (Quevedo et al., 1998). It is possible that the female mice used in our experiments could have been cold acclimated from living at room temperature and therefore, do not show as high of a response to the room temperature condition as seen in other research. Therefore, more research needs to be done to understand whether sex has an effect on thermoregulatory mechanisms.

Similarly, we investigated whether the time of day had an effect on levels of thermogenesis. Mice undergoing the anticipatory cold-context association protocol either during the daytime or the night time showed a difference in the timing of increases and decreases in the rate of EE, which is what we would expect based on our knowledge of circadian rhythms. As core body temperature and activity levels fluctuate throughout a 24-hour cycle, the EE rate reflects these changes. The results from this experiment do not show a significant difference in the rate of EE or UCP-1 mRNA levels in daytime compared to night time.

This result would suggest that there is not a significant influence of time of day on thermogenesis levels, in both cold and room temperature conditions. However, there are clearly differences in the timing of increases and decrease in EE during daytime and night-time and therefore further investigation could focus on the interaction between variables affecting EE, such as core body temperature, based on the influence of circadian rhythms.

4.4 Extended effect of cold exposure on thermogenesis

Additionally, this project has provided information on how long the effects of cold exposure can last for. Previous research shows that BAT mRNA levels peak after 6 hours in the cold and then decrease as cold exposure continues (Nedergaard and Cannon, 2013). But research has not yet clarified if thermogenesis remains higher after cold exposure even when mice are placed back at room temperature instead of given continuous cold exposure.

Our results show that 3 days of cold exposure can have an extended thermogenic effect for at least 16 hours after exposure. The increased UCP-1 mRNA levels signifying a thermogenic effect are seen 16 hours after cold exposure but decrease by 40 hours post-exposure. However, this experimental design lacks a pre-exposure UCP-1 mRNA quantification and therefore does not provide conclusive evidence that the level of thermogenesis has returned to pre-exposure conditions at 40 hours post-exposure. Further research could be done to clarify the exact amount of time required after cold exposure to allow for the UCP-1 mRNA to reach pre-exposure levels, signifying that there is no longer a thermogenic effect.

Additionally, this research acknowledges that UCP-1 mRNA levels do not solely represent the magnitude of thermogenesis activation. Therefore, the rate of EE was also measured to understand whether metabolic effects of thermogenesis were present. The rate of EE 16 hours post-exposure was higher than 40 hours post-exposure. This metabolic data supports our conclusion that the thermogenic effect of cold exposure lasts for at least 16 hours and decreases by 40 hours post-exposure.

4.5 Future directions

One main goal of this project was to adapt the engram-labelling technique to be used in temperature research. The temporal and spatial specificity provided by engram labelling could benefit thermoregulation research by providing information about the characteristics of temperature-sensitive neurons and the circuits involved in thermoregulation. While this project was unsuccessful in labelling temperature-sensitive neurons using the engram labelling technique, there is still potential for this technique to be useful for temperature research. Future investigation could focus on

optimisation of the target area, as well as the length of exposure in order to develop this technique properly in the given application.

Another objective of this research was to better understand the different factors influencing thermoregulation. Our results show that neither sex nor time of day have a significant influence on the levels of thermogenesis or EE in both room temperature and cold conditions. However, this research only addressed EE and UCP-1 mRNA levels to understand thermogenesis, while in reality there are many additional influences on thermoregulatory mechanisms. Therefore, future research could focus on different metabolic and behavioural thermoregulatory responses to provide a broader understanding of the thermoregulatory system in mammals.

Finally, this research has provided a novel protocol for investigating the influence of memory on thermoregulation. Our results indicate that mice can associate a context with a temperature, and that the context alone is sufficient to elicit metabolic responses seen in natural temperature exposure. These results provide a foundation to investigate the mechanisms through which thermoregulatory responses are initiated by memory in the absence of natural cues. One limitation of this protocol is that the temperature ramp on the cold days is introduced immediately after the animal enters the context. To improve on this, future experiments could add a short period at the beginning of the exposure where the animal experiences the context alone without the temperature ramp. This context-only period would provide definitive results as to whether a context memory can elicit metabolic responses.

The results from this research provide preliminary evidence for the role of memory in thermoregulation. This finding opens up many opportunities for future research into the interaction between memory and innate responses. Future research could investigate whether optogenetically reactivating the contextual engram for a temperature exposure can elicit metabolic responses seen in the natural temperature condition. Another potential direction is to investigate whether innate temperature responses can be modulated by learning and memory. This avenue would be particularly interesting for investigating treatments for thermoregulatory deficiencies. It would also provide a platform to interrogate the potential of shared encoding mechanisms in the brain

between innate and learned information. In conclusion, this research provides a foundation for further investigation of innate temperature representations in the brain.

Bibliography

ALLEN, W. E., DENARDO, L. A., CHEN, M. Z., LIU, C. D., LOH, K. M., FENNO, L. E., RAMAKRISHNAN, C., DEISSEROTH, K. & LUO, L. 2017. Thirst-associated preoptic neurons encode an aversive motivational drive. *Science,* 357**,** 1149-1155.

ALMEIDA, M. C., VIZIN, R. C. & CARRETTIERO, D. C. 2015. Current understanding on the neurophysiology of behavioral thermoregulation. *Temperature (Austin),* 2**,** 483-90.

ARAVANIS, A. M., WANG, L. P., ZHANG, F., MELTZER, L. A., MOGRI, M. Z., SCHNEIDER, M. B. & DEISSEROTH, K. 2007. An optical neural interface: in vivo control of rodent motor cortex with integrated fiberoptic and optogenetic technology. *J Neural Eng,* 4**,** S143-56.

AVRAM, A. S., AVRAM, M. M. & JAMES, W. D. 2005. Subcutaneous fat in normal and diseased states: 2. Anatomy and physiology of white and brown adipose tissue. *J Am Acad Dermatol,* 53**,** 671-83.

BANET, M., HENSEL, H. & LIEBERMANN, H. 1978. The central control of shivering and non-shivering thermogenesis in the rat. *J Physiol,* 283**,** 569-84.

BAUTISTA, D. M., SIEMENS, J., GLAZER, J. M., TSURUDA, P. R., BASBAUM, A. I., STUCKY, C. L., JORDT, S. E. & JULIUS, D. 2007. The menthol receptor TRPM8 is the principal detector of environmental cold. *Nature,* 448**,** 204-8.

BOULANT, J. A. & BIGNALL, K. E. 1973. Hypothalamic neuronal responses to peripheral and deep-body temperatures. *Am J Physiol,* 225**,** 1371-4.

BOULANT, J. A. & HARDY, J. D. 1974. The effect of spinal and skin temperatures on the firing rate and thermosensitivity of preoptic neurones. *J Physiol,* 240**,** 639-60.

BRATINCSAK, A. & PALKOVITS, M. 2004. Activation of brain areas in rat following warm and cold ambient exposure. *Neuroscience,* 127**,** 385-97.

BRATINCSAK, A. & PALKOVITS, M. 2005. Evidence that peripheral rather than intracranial thermal signals induce thermoregulation. *Neuroscience,* 135**,** 525-32.

BULLITT, E. 1990. Expression of c-fos-like protein as a marker for neuronal activity following noxious stimulation in the rat. *J Comp Neurol,* 296**,** 517-30.

CANNON, B. & NEDERGAARD, J. 2004. Brown adipose tissue: function and physiological significance. *Physiol Rev,* 84**,** 277-359.

CAZZULINO, A. S., MARTINEZ, R., TOMM, N. K. & DENNY, C. A. 2016. Improved specificity of hippocampal memory trace labeling. *Hippocampus,* 26**,** 752-62.

CHEN, X. M., HOSONO, T., YODA, T., FUKUDA, Y. & KANOSUE, K. 1998. Efferent projection from the preoptic area for the control of non-shivering thermogenesis in rats. *J Physiol,* 512 (Pt 3)**,** 883-92.

DEGEN, A. A., KAM, M., KHOKHLOVA, I. S., KRASNOV, B. R. & BARRACLOUGH, T. G. 1998. Average daily metabolic rate of rodents: habitat and dietary comparisons. *Functional Ecology,* 12**,** 63–73.

DHAKA, A., VISWANATH, V. & PATAPOUTIAN, A. 2006. Trp ion channels and temperature sensation. *Annu Rev Neurosci,* 29**,** 135-61.

FENNO, L., YIZHAR, O. & DEISSEROTH, K. 2011. The development and application of optogenetics. *Annu Rev Neurosci,* 34**,** 389-412.
GASKILL, B. N., GORDON, C. J., PAJOR, E. A., LUCAS, J. R., DAVIS, J. K. & GARNER, J. P. 2012. Heat or insulation: behavioral titration of mouse preference for warmth or access to a nest. *PLoS One,* 7**,** e32799.
GASKILL, B. N., ROHR, S. A., PAJOR, E. A., LUCAS, J. R. & GARNER, J. P. 2008. Some like it hot: Mouse temperature preferences in laboratory housing. *Applied Animal Behaviour Science,* 116 (2)**,** 279-285.
GODSIL, B. P., QUINN, J. J. & FANSELOW, M. S. 2000. Body temperature as a conditional response measure for pavlovian fear conditioning. *Learn Mem,* 7**,** 353-6.
GORDON, C. J. 2009. Quantifying the instability of core temperature in rodents. *Journal of Thermal Biology,* 34**,** 213-219.
GORDON, C. J. 2017. The mouse thermoregulatory system: Its impact on translating biomedical data to humans. *Physiol Behav,* 179**,** 55-66.
GORDON, C. J., BECKER, P. & ALI, J. S. 1998. Behavioral thermoregulatory responses of single- and group-housed mice. *Physiol Behav,* 65**,** 255-62.
GOVORUNOVA, E. G., SINESHCHEKOV, O. A., JANZ, R., LIU, X. & SPUDICH, J. L. 2015. NEUROSCIENCE. Natural light-gated anion channels: A family of microbial rhodopsins for advanced optogenetics. *Science,* 349**,** 647-50.
HAMMEL, H. T. 1968. Regulation of internal body temperature. *Annu Rev Physiol,* 30**,** 641-710.
HANKENSON, F. C., MARX, J. O., GORDON, C. J. & DAVID, J. M. 2018. Effects of Rodent Thermoregulation on Animal Models in the Research Environment. *Comp Med,* 68**,** 425-438.
HAWKINS, P. & GOLLEDGE, H. D. R. 2018. The 9 to 5 Rodent - Time for Change? Scientific and animal welfare implications of circadian and light effects on laboratory mice and rats. *J Neurosci Methods,* 300**,** 20-25.
HIMMS-HAGEN, J. 2001. Does brown adipose tissue (BAT) have a role in the physiology or treatment of human obesity? *Rev Endocr Metab Disord,* 2**,** 395-401.
HORI, T. 1991. An update on thermosensitive neurons in the brain: from cellular biology to thermal and non-thermal homeostatic functions. *Jpn J Physiol,* 41**,** 1-22.
KAIKAEW, K., STEENBERGEN, J., THEMMEN, A. P. N., VISSER, J. A. & GREFHORST, A. 2017. Sex difference in thermal preference of adult mice does not depend on presence of the gonads. *Biol Sex Differ,* 8**,** 24.
KAIYALA, K. J., WISSE, B. E. & LIGHTON, J. R. B. 2019. Validation of an equation for energy expenditure that does not require the respiratory quotient. *PLoS One,* 14**,** e0211585.
LEIN, E. S., HAWRYLYCZ, M. J., AO, N., AYRES, M., BENSINGER, A., BERNARD, A., BOE, A. F., BOGUSKI, M. S., BROCKWAY, K. S., BYRNES, E. J., CHEN, L., CHEN, L., CHEN, T. M., CHIN, M. C., CHONG, J., CROOK, B. E., CZAPLINSKA, A., DANG, C. N., DATTA, S., DEE, N. R., DESAKI, A. L., DESTA, T., DIEP, E., DOLBEARE, T. A., DONELAN, M. J., DONG, H. W., DOUGHERTY, J. G., DUNCAN, B. J., EBBERT, A. J., EICHELE, G., ESTIN, L. K., FABER, C., FACER, B. A., FIELDS, R., FISCHER, S. R., FLISS, T. P., FRENSLEY, C., GATES, S. N., GLATTFELDER, K. J., HALVERSON, K. R., HART, M. R., HOHMANN, J. G., HOWELL, M. P., JEUNG, D. P., JOHNSON, R. A., KARR, P. T.,

KAWAL, R., KIDNEY, J. M., KNAPIK, R. H., KUAN, C. L., LAKE, J. H., LARAMEE, A. R., LARSEN, K. D., LAU, C., LEMON, T. A., LIANG, A. J., LIU, Y., LUONG, L. T., MICHAELS, J., MORGAN, J. J., MORGAN, R. J., MORTRUD, M. T., MOSQUEDA, N. F., NG, L. L., NG, R., ORTA, G. J., OVERLY, C. C., PAK, T. H., PARRY, S. E., PATHAK, S. D., PEARSON, O. C., PUCHALSKI, R. B., RILEY, Z. L., ROCKETT, H. R., ROWLAND, S. A., ROYALL, J. J., RUIZ, M. J., SARNO, N. R., SCHAFFNIT, K., SHAPOVALOVA, N. V., SIVISAY, T., SLAUGHTERBECK, C. R., SMITH, S. C., SMITH, K. A., SMITH, B. I., SODT, A. J., STEWART, N. N., STUMPF, K. R., SUNKIN, S. M., SUTRAM, M., TAM, A., TEEMER, C. D., THALLER, C., THOMPSON, C. L., VARNAM, L. R., VISEL, A., WHITLOCK, R. M., WOHNOUTKA, P. E., WOLKEY, C. K., WONG, V. Y., et al. 2007. Genome-wide atlas of gene expression in the adult mouse brain. *Nature,* 445**,** 168-76.

LIEDTKE, W. B. 2017. Deconstructing mammalian thermoregulation. *Proc Natl Acad Sci U S A,* 114**,** 1765-1767.

LIU, X., RAMIREZ, S., PANG, P. T., PURYEAR, C. B., GOVINDARAJAN, A., DEISSEROTH, K. & TONEGAWA, S. 2012. Optogenetic stimulation of a hippocampal engram activates fear memory recall. *Nature,* 484**,** 381-5.

LIU, X., RAMIREZ, S. & TONEGAWA, S. 2014. Inception of a false memory by optogenetic manipulation of a hippocampal memory engram. *Philos Trans R Soc Lond B Biol Sci,* 369**,** 20130142.

LYNCH, G. R., LYNCH, C. B., DUBE, M. & ALLEN, C. 1976. Early Cold Exposure: Effects on Behavioral and Physiological Thermoregulation in the House Mouse, Mus musculus. *Physiological Zoology,* 49(2)**,** 191-199.

MADDEN, C. J. & MORRISON, S. F. 2019. Central nervous system circuits that control body temperature. *Neurosci Lett,* 696**,** 225-232.

MADISEN, L., MAO, T., KOCH, H., ZHUO, J. M., BERENYI, A., FUJISAWA, S., HSU, Y. W., GARCIA, A. J., 3RD, GU, X., ZANELLA, S., KIDNEY, J., GU, H., MAO, Y., HOOKS, B. M., BOYDEN, E. S., BUZSAKI, G., RAMIREZ, J. M., JONES, A. R., SVOBODA, K., HAN, X., TURNER, E. E. & ZENG, H. 2012. A toolbox of Cre-dependent optogenetic transgenic mice for light-induced activation and silencing. *Nat Neurosci,* 15**,** 793-802.

MINA, A. I., LECLAIR, R. A., LECLAIR, K. B., COHEN, D. E., LANTIER, L. & BANKS, A. S. 2018. CalR: A Web-Based Analysis Tool for Indirect Calorimetry Experiments. *Cell Metab,* 28**,** 656-666 e1.

MORRISON, S. F. & NAKAMURA, K. 2019. Central Mechanisms for Thermoregulation. *Annu Rev Physiol,* 81**,** 285-308.

NAKAMURA, K. & MORRISON, S. F. 2008. Preoptic mechanism for cold-defensive responses to skin cooling. *J Physiol,* 586**,** 2611-20.

NEDERGAARD, J. & CANNON, B. 2013. UCP1 mRNA does not produce heat. *Biochim Biophys Acta,* 1831**,** 943-9.

ORDAS, P., HERNANDEZ-ORTEGO, P., VARA, H., FERNANDEZ-PENA, C., REIMUNDEZ, A., MORENILLA-PALAO, C., GUADANO-FERRAZ, A., GOMIS, A., HOON, M., VIANA, F. & SENARIS, R. 2019. Expression of the cold thermoreceptor TRPM8 in rodent brain thermoregulatory circuits. *J Comp Neurol*.

QUEVEDO, S., ROCA, P., PICO, C. & PALOU, A. 1998. Sex-associated differences in cold-induced UCP1 synthesis in rodent brown adipose tissue. *Pflugers Arch,* 436**,** 689-95.

RAETZ, C., PERRY, A., PRIBIL, B., COBBS, M. 2015. Mouse: Temperature vs Cellular Respiration Rate. *Journal of Introductory Biology Investigations,* 2.
REITMAN, M. L. 2018. Of mice and men - environmental temperature, body temperature, and treatment of obesity. *FEBS Lett,* 592**,** 2098-2107.
RIEDE, S. J., VAN DER VINNE, V. & HUT, R. A. 2017. The flexible clock: predictive and reactive homeostasis, energy balance and the circadian regulation of sleep-wake timing. *J Exp Biol,* 220**,** 738-749.
RYAN, T. J. 2020. Memory and Instinct as a Continuum of Information Storage. *In:* POEPPEL, D., MANGUN, G.R., GAZZANIGA, M.S. (ed.) *The Cognitive Neurosciences.* Cambridge, MA: The MIT Press.
RYAN, T. J., ROY, D. S., PIGNATELLI, M., ARONS, A. & TONEGAWA, S. 2015. Memory. Engram cells retain memory under retrograde amnesia. *Science,* 348**,** 1007-13.
SHABTAY, A. & ARAD, Z. 2005. Ectothermy and endothermy: evolutionary perspectives of thermoprotection by HSPs. *J Exp Biol,* 208**,** 2773-81.
SHORE, A. M., KARAMITRI, A., KEMP, P., SPEAKMAN, J. R., GRAHAM, N. S. & LOMAX, M. A. 2013. Cold-induced changes in gene expression in brown adipose tissue, white adipose tissue and liver. *PLoS One,* 8**,** e68933.
SIMON, H. B. 1993. Hyperthermia. *N Engl J Med,* 329**,** 483-7.
SPEAKMAN, J. R. 2013. Measuring energy metabolism in the mouse - theoretical, practical, and analytical considerations. *Front Physiol,* 4**,** 34.
TAN, C. L. & KNIGHT, Z. A. 2018. Regulation of Body Temperature by the Nervous System. *Neuron,* 98**,** 31-48.
TANAKA, K. Z., PEVZNER, A., HAMIDI, A. B., NAKAZAWA, Y., GRAHAM, J. & WILTGEN, B. J. 2014. Cortical representations are reinstated by the hippocampus during memory retrieval. *Neuron,* 84**,** 347-54.
TANSEY, E. A. & JOHNSON, C. D. 2015. Recent advances in thermoregulation. *Adv Physiol Educ,* 39**,** 139-48.
TERRIEN, J., PERRET, M. & AUJARD, F. 2011. Behavioral thermoregulation in mammals: a review. *Front Biosci (Landmark Ed),* 16**,** 1428-44.
TINBERGEN, N. 1951. *The Study Of Instinct,* Oxford: Clarendon Press.
VAN DER VINNE, V., GORTER, J. A., RIEDE, S. J. & HUT, R. A. 2015. Diurnality as an energy-saving strategy: energetic consequences of temporal niche switching in small mammals. *J Exp Biol,* 218**,** 2585-93.
VIANNA, D. M. & CARRIVE, P. 2005. Changes in cutaneous and body temperature during and after conditioned fear to context in the rat. *Eur J Neurosci,* 21**,** 2505-12.
WEIR, J. B. 1949. New methods for calculating metabolic rate with special reference to protein metabolism. *J Physiol,* 109**,** 1-9.
ZHANG, Y. H., YANASE-FUJIWARA, M., HOSONO, T. & KANOSUE, K. 1995. Warm and cold signals from the preoptic area: which contribute more to the control of shivering in rats? *J Physiol,* 485 (Pt 1)**,** 195-202.
ZHAO, Z. D., YANG, W. Z., GAO, C., FU, X., ZHANG, W., ZHOU, Q., CHEN, W., NI, X., LIN, J. K., YANG, J., XU, X. H. & SHEN, W. L. 2017. A hypothalamic circuit that controls body temperature. *Proc Natl Acad Sci U S A,* 114**,** 2042-2047.